

Considerations from the Innovation and Quality Induction Working Group in Response to Drug-Drug Interaction Guidance from Regulatory Agencies: Guidelines on Model Fitting and Recommendations on Time Course for In Vitro CYP Induction Studies Including Impact on Drug Interaction Risk Assessment

Simon G. Wong, Diane Ramsden, Shannon Dallas, Conrad Fung, Heidi J. Einolf, Jairam Palamanda, Liangfu Chen, Theunis C. Goosen, Y. Amy Siu, George Zhang, Donald Tweedie, Nireesh Hariparsad, Barry Jones, and Phillip D. Yates.

Affiliations

Genentech, South San Francisco, California (SGW); Alnylam Pharmaceuticals, Cambridge, Massachusetts (DR); Janssen R&D, Spring House, Pennsylvania (SD); Vertex Pharmaceuticals, Boston, Massachusetts (NH,CF); Novartis, East Hanover, New Jersey (HJE); GlaxoSmithKline, King of Prussia, Pennsylvania (L.C); Pfizer Global Research and Development, Groton, Connecticut (TCG), & Cambridge, Massachusetts (PDY); Eisai, Cambridge Massachusetts (AS), Corning Life Sciences, Woburn, Massachusetts (GZ); Merck & Co., Inc., Kenilworth, New Jersey (DT, JP); Astra Zeneca, Cambridge, Cambridgeshire, UK (BJ);

Current Affiliations

Pliant Therapeutics, South San Francisco (SGW); Takeda, Cambridge Massachusetts (DR); SK Life Sciences, Paramus, New Jersey (JP); AbbVie, Worcester Massachusetts (AS); Pharmaron, Rushden, UK (BJ); AstraZeneca, 35 Gatehouse Dr, Waltham, MA 02451 (NH); Bristol Myers Squibb, New Brunswick, New Jersey (PDY).

Running title: Time Course for CYP induction and guidelines for model fitting

Corresponding Author:

Niresh Hariparsad

AstraZeneca

35 Gatehouse Dr, Waltham, MA 02451

Email: Niresh.hariparsad@astrazeneca.com

Number of Text Pages: 66

Number of Tables: 7

Number of Figures: 8

Number of References: 39

Number of words in Abstract: 250 (≤ 250)

Number of words in Introduction: 591 (< 750)

Number of words in Discussion: 1720 (< 1800)

Supplementary Tables/Figures: 2/4

Abbreviations: CYP, cytochrome P450; DDI (drug-drug interaction); FDA, Food and Drug Administration; EMA, European Medicines Agency; PDMA, Pharmaceutical and Medical Devices Agency; TALG, Translational ADME Sciences Leadership Group; IWG, Induction Working Group; CITCO, (6-(4chlorophenyl)imidazo[2,1-b][1,3]thiazole-5-carbaldehyde-O-(3,4dichlorobenzyl)oxime); E_{\max} , maximal-fold induction (fitted), EC_{50} , concentration eliciting half-maximal fold induction; DMSO, dimethyl sulfoxide; PCR, polymerase chain reaction; AICc, Akaike's information criteria; AFE, average fold error; I_u , unbound inducer concentration

Abstract

Translational and ADME Sciences Leadership Group (TALG) Induction Working Group (IWG) presents an analysis on the time-course for cytochrome P450 induction in primary human hepatocytes. Induction of CYP1A2, CYP2B6, and CYP3A4 was evaluated by seven IWG laboratories following incubation with prototypical inducers (omeprazole, phenobarbital, rifampicin, and efavirenz) for 6 to 72 hours. The effect of incubation duration and model-fitting approaches on induction parameters (E_{\max} and EC_{50}) and drug-drug interaction (DDI) risk assessment was determined. Despite variability in induction response across hepatocyte donors, the following recommendations are proposed: i) 48 hours should be the primary time point for in vitro assessment of induction, based on mRNA level or activity, with no further benefit from 72 hours, ii) when using mRNA, 24 hour incubations provide reliable assessment of induction and DDI risk, iii) if validated using prototypical inducers (>10-fold induction), 12-hour incubations may provide an estimate of induction potential including characterization as negative if < 2-fold induction of mRNA and no concentration-dependence, iv) atypical dose-response ('bell-shaped') curves can be addressed by removing points outside an established confidence interval and %CV, v) when maximum fold induction is well-defined, the choice of non-linear regression model has limited impact on estimated induction parameters, vi) when the maximum-fold induction is not well-defined, conservative DDI risk assessment can be obtained using sigmoidal-3-parameter fit or constraining logistic 3/4 parameter fits to the maximum observed fold induction, vii) preliminary data suggest initial slope of the fold induction curve can be used to estimate E_{\max}/EC_{50} and for induction risk assessment.

Significance Statement

Global Regulatory agencies have provided inconsistent guidance on the optimum length of time to evaluate CYP induction in human hepatocytes, with the EMA recommending 72 h and the FDA suggesting 48 to 72 h. The IWG analyzed a large dataset generated by 7 member companies and determined that induction response and drug-drug risk assessment determined after 48 h incubations was representative of 72 h incubations. Additional recommendations are provided on model-fitting techniques for induction parameter estimation and addressing atypical concentration-response curves.

Introduction

Regulatory agencies continue to update and evolve their guidance's for the conduct of in vitro studies to evaluate the propensity for induction-mediated drug-drug interactions (DDIs). The final guidance¹ released by the Food and Drug Administration (FDA) in early 2020, in addition to the latest guidance² (2012) from the European Medicines Agency (EMA) and Pharmaceutical and Medical Devices Agency (PDMA)³ (2014; Finalized in 2018) provided recommendations on the conduct, interpretation, and risk-assessment for the likelihood of a clinical DDI arising from CYP induction. The Translational and ADME Sciences Leadership Group (TALG) Induction Working Group (IWG) has previously commented on CYP induction and the regulatory guidance. Hariparsad et al. (2017) presented results from an industry survey related to induction evaluation and provided data driven recommendations on the evaluation of CYP downregulation, in vitro assessment of CYP2C induction, and the use of CITCO (6-(4chlorophenyl)imidazo[2,1-b][1,3]thiazole-5-carbaldehyde-O-(3,4dichlorobenzyl)oxime) as a positive control for CYP2B6. In a follow-up manuscript, Kenny et al (2018) provided an extensive analysis of CYP3A4 induction response, thresholds, and variability and made key recommendations related to number of donors, criteria for characterizing positive and negative in vitro induction including the 2-fold cut-off, the value of negative controls, and finally indexing response to prototypical inducers. More recently, Ramsden et al (2019) sought to identify contributors to variable outcomes in clinical DDI induction data and methods for understanding how these factors impact characterization of induction.

The appropriate duration of incubation of hepatocytes with test article was identified as an area requiring further exploration and remains a topic of high interest. Of note, recommendations from the regulatory agencies are inconsistent: the FDA recommends incubations of 48 to 72 h,

whereas the EMA requires clear justification for incubations less than 72 h. To this end, the IWG sought to evaluate the appropriate incubation time with human hepatocytes to adequately assess CYP induction. In 2007, a survey of the pharmaceutical industry indicated that assessment of CYP induction is routinely conducted after 48 h (73% of the respondents), with some investigators using even shorter incubations (Hewitt et al., 2007). This observation was replicated in a subsequent survey conducted by the IWG, ten years later, where 71% of respondents indicated that they also used 48 h as the primary incubation time despite the EMA guideline, released in 2012, proposing 72 h (Hariparsad et al., 2017). Member companies justified this based on their historical data and the switch from enzyme activity to mRNA as the primary endpoint for evaluating induction potential. The utility of shorter incubations for the assessment of CYP induction can be particularly advantageous in cases where prolonged exposure of higher test article concentration results in cytotoxicity, which prevents reliable determination of the key induction parameters, EC_{50} (the concentration eliciting half-maximal induction) and E_{max} (the maximum fold induction). This strategy was successfully applied by Sane et al. (2016), who monitored changes in mRNA levels following a short incubation (10 h) in hepatocytes to assess the risk for induction-mediated DDI's caused by deleobuvir, which was cytotoxic after 24 or 48 h.

Recognizing the value in establishing the relationship between incubation duration, induction response, and DDI-risk assessment, the primary objective of the present study was to characterize the time-course of CYP induction in human hepatocytes after treatment with prototypical inducers (omeprazole, phenobarbital, efavirenz, or rifampicin) and determine the optimal incubation time for induction DDI risk assessment. In order to enable comparison of induction response across the seven IWG laboratories participating in this study, a secondary

objective was to examine the feasibility of describing a consistent approach towards induction data processing and model fitting.

Materials and Methods

Reagents. Bupropion, efavirenz, phenobarbital, omeprazole, phenacetin, acetaminophen, hydroxybupropion, 1'OH midazolam and rifampicin were purchased from Sigma-Aldrich (St. Louis, MO). Midazolam was purchased from Cerilliant (Round Rock, TX). Isotopically labeled internal metabolite standards were purchased from Corning Life Sciences (Woburn, MA). The RNeasy Mini Kit was from Qiagen (Valencia, CA) and the cDNA Reverse Transcription Kit was obtained from Applied Biosystems (Foster City, CA). All cell culture reagents were purchased from Life Technologies, BioIVT, Lonza or Corning Life Sciences unless otherwise noted. Reagents were not standardized for consistency across laboratories, but were of highest purity and chemical grade, and potential differences were not expected to affect the overall induction response.

Culture of Cryopreserved Human Hepatocytes

Human cryopreserved hepatocytes, from both males and females of different ages and racial origin, were obtained from several commercial vendors (Supplementary Table 1): CellzDirect (Durham, NC), Thermo Fisher (Waltham, MA), Bioreclamation In Vitro Technologies (Baltimore, MD), Corning Life Sciences (Woburn, MA) and XenoTech LLC, (Kansas City, KS). To better represent data provided during regulatory reviews, participating labs used their standard procedures and no modifications or standardizations of procedures were suggested. A standardized approach for model-fitting and estimation of induction parameters E_{\max} and EC_{50} , however, was employed to ensure consistent DDI risk assessment across all 7 member laboratories. As detailed in previous publications (Fahmi and Ripp, 2010; Zhang et al., 2014; Sane et al., 2016; Sun et al., 2017) cryopreserved human hepatocytes were thawed in hepatocyte thawing medium and were seeded in collagen I coated 24- or 96-well plates at cell densities of

0.5 to 1×10^6 viable cells per mL in hepatocyte plating medium. Viability, as determined by trypan blue dye exclusion, was at least 85% when cells were plated. Cells were initially maintained overnight at 37°C in a humidified incubator, with 95% atmospheric air and 5% CO₂, in hepatocyte incubation media. Following individual lab standard acclimation periods (24 to 48 h), the cells were treated with compounds. When sandwich cultured hepatocytes were used, cells were overlaid with matrigel between 4-24 h post attachment, maintained for an additional 24 h under incubated settings and then treated with compounds. Compounds were dissolved in DMSO and added to the culture medium at various concentrations (final DMSO concentration, 0.1%, Supplementary Table 2) in triplicate. Wells containing 0.1% DMSO only were included as controls. The concentration range was designed to adequately describe the induction parameters by considering published induction parameters, historical data within the IWG and solubility/cytotoxicity limitations for the inducers. Media was aspirated and replaced with fresh media containing inducers every 24 h for 24 to 72 h treatment plates. Cell viability was assessed by visual inspection of the monolayer, checking for confluency and morphology. After designated treatment time (6, 12, 24, 48 or 72 h), the medium was removed, and the cells were washed with an appropriate buffer (i.e. PBS or HBSS).

Determination of Relative mRNA Levels

The cells were lysed using lysis buffer and prepared for RNA isolation. After the isolation of RNA using commercially available kits, cDNA was synthesized using standard polymerase chain reaction (PCR) protocols. CYP (1A2, 2B6, 2C8, 2C9, 2C19 and 3A4), and an endogenous housekeeping gene control (e.g., glyceraldehyde-3- phosphate dehydrogenase, β -actin, or β 2-microglobulin) were quantified by real-time PCR. The gene-specific primer/probe sets were obtained from Applied Biosystems and real-time PCR was performed using CYP (1A2, 2B6,

2C8, 2C9, 2C19 and 3A4), and the endogenous control target cDNAs. The relative quantity of the target cDNA compared with that of the endogenous control was determined by the $\Delta\Delta$ threshold cycle method (Applied Biosystems User Bulletin 2). Threshold cycle values > 32 were excluded from the analysis. Relative quantification measured the change in mRNA expression in test samples relative to that in vehicle control sample (0.1% DMSO).

Determination of Relative Enzyme Activity

After designated treatment times, hepatocyte cultures were washed and incubated with single or cocktail probe substrates (phenacetin, bupropion, and/or midazolam), according to individual company standard practices. All enzyme activities were determined by measuring the metabolite formation of the specific probe substrate for each enzyme. The standard curves with single metabolite or cocktail metabolites were prepared and analyzed by LC-MS/MS for single and cocktail assays, respectively. Note that CYP2C activity was not determined in the present study due to the low dynamic range in response (Hariparsad et al., 2017).

Model Fitting Fold Induction Data

Detailed description of the methods employed for model fitting fold induction data are described below, and the results of various approaches are reviewed in the results and discussion sections. Explicit guidelines for initial data inspection and quality control concerns are not provided. Consistent with the need to evaluate for potential outliers (Reference USP 1032) and their effect on subsequent analyses, for the analyses presented here triplicate samples were excluded from curve fitting if the CV was greater than 30% (approximately 10% for mRNA and 4% for activity). In general, traditional statistical outlier tests (e.g., Grubb's), readily available in some

commercial software tools, are not recommended to identify potential outliers from triplicate data due to small sample sizes (Laio, 2010).

Confirmation of Concentration Dependence Prior to Curve Fitting

To reduce curve fitting attempts for weak or highly variable fold induction data and its impact on the DDI risk assessment, an initial statistical procedure for demonstrating a concentration-dependence is suggested. Two methods were used to evaluate concentration dependence: standard linear regression and Spearman's nonparametric rank correlation coefficient. If either method indicated a statistically significant increase (i.e a non-zero slope/correlation) then non-linear regression curve fitting was performed. This step was adopted from a decision tree to evaluate time dependent inhibitors, another DDI risk component that can involve design or curve fitting challenges (Yates et al., 2012).

Curve Fitting Fold Induction Data and Estimation of Induction Parameters E_{\max} and EC_{50}

In vitro concentration-response data, based on mRNA or activity, were generated by 7 IWG member companies. Each inducer-isoform pair was investigated in a single experiment at each lab, with each concentration of inducer evaluated in triplicate. Induction parameters E_{\max} and EC_{50} were determined by plotting the in vitro fold induction data (mRNA or enzyme activity normalized to the control) against the nominal in vitro concentration and analyzed using non-linear regression models in GraphPad Prism (Version 8). To the best of our knowledge only empirical models are available and routinely estimated for induction. A consistent feature of these models is the assumed presence of a fold induction plateau, i.e., E_{\max} . Since different labs historically used a variety of different non-linear regression models, 5 non-linear regression models were evaluated:

Equation 1: Logistic 3P Equation (Log(Agonist) vs Response (3 Parameter))

(1)

$$y = bottom + \frac{Emax - bottom}{1 + 10^{Log(EC_{50} - [I])}}$$

Equation 2: Logistic 4P Equation (Log(Agonist) vs Response (4 Parameter))

(2)

$$y = bottom + \frac{Emax - bottom}{1 + 10^{Log(EC_{50} - [I]) * h}}$$

Equation 3: Sigmoidal 3-Parameter

(3)

$$y = \frac{E_{max}}{1 + e^{\left[\frac{-([I] - EC_{50})}{h} \right]}}$$

Equation 4: E_{max} Model (Hill Model)

(4)

$$y = \frac{E_{max} \times [I]^h}{EC_{50}^h + [I]^h}$$

Equation 5: Hyperbolic Model (One Site)

(5)

$$y = \frac{E_{max} \times [I]}{EC_{50} + [I]}$$

For all models, y = relative fold induction, $[I]$ is the test article concentration, EC_{50} is the concentration eliciting half-maximal induction, and E_{max} is the maximum fold induction. For equations 1 and 2, bottom is the lowest fold induction and is constrained to a value of 1.0 (i.e., induction response is normalized to vehicle control, where 1.0-fold induction is baseline, or no induction). For equations 2, 3, and 4, h is the Hill slope. Model estimates were reported when the standard error of the estimate was less than 50% of the model estimate. Model fits were compared using small sample-size corrected Akaike's information criteria (AICc) (Burnham and Anderson, 2002) and AICc weight (Wagenmakers and Farrell, 2004). The default equation used for comparison of induction parameters determined at different time points was equation 1 (Logistic 3P equation); in cases where the maximum fold induction was not achieved, equation 3 (Sigmoidal 3P equation) was used. See results section "Comparison of Non-linear Regression Models For Estimation of E_{max} and EC_{50} from Fold Induction Data " for additional details on this approach.

Estimation of E_{max}/EC_{50} Using Linearization (Initial Slope Approaches)

The initial slope of the fold induction vs concentration curve, at low concentrations typically less than the EC_{30} , can provide an estimation of E_{max}/EC_{50} , under the assumptions suitable for such a simplified model (Shou et al., 2008). It is important to note that this relationship is only applicable if in vivo concentrations of the inducer are low ($[I] \ll EC_{50}$), and the initial slope is determined by linear regression of the fold induction vs (non-log) concentration. To investigate this approach to estimate E_{max}/EC_{50} , the following criteria were implemented: slope determined using at least 4 data points, with at least one yielding >2-fold induction response. Initial slopes were reported when $R^2 > 0.9$ and the standard error of the slope was less than 50% of the estimated slope.

Comparison of Model Estimates Determined at 6, 12, 24 or 48 Hours with Model Estimates Determined at 72 Hours

To examine the relationship between incubation duration and time, fold error was determined by comparing the parameter estimates obtained at 72 h with those obtained at earlier time points.

Overall average fold error (AFE) between parameter estimates (i.e. E_{\max} or EC_{50}) determined at earlier time points (6, 12, 24, or 48 h) and 72 h was calculated using equation 6:

(6)

$$AFE = 10^{\sum \frac{\log_{10} \left(\frac{6,12,24 \text{ or } 48 \text{ hr estimate}}{72 \text{ hr estimate}} \right)}{\# \text{ of samples}}}$$

Calculation of AFE was paired such that parameter estimates of E_{\max} or EC_{50} at 72 h were compared to the parameter estimates generated by the same laboratory at early time points (6, 12, 24 or 48 h).

Prediction of In vivo DDI

The change in exposure of a victim drug due to CYP induction was predicted using the following steady-state approaches (equations 7 to 9):

(7)

$$AUCr = \frac{1}{1 + \frac{E_{\max} \times [I_u]}{EC_{50} + [I_u]}} e$$

$[I_u]$ is the unbound inducer concentration.

Equation 8 eliminates the need of individually determined E_{\max} and EC_{50} values and instead uses a combined term, E_{\max}/EC_{50} . Note that this approximation is only true when $[I_u] \ll EC_{50}$.

(8)

$$AUCr = \frac{1}{1 + \frac{Emax}{EC50} \times [I_u]}$$

Equation 9 uses the slope of the fold induction vs concentration estimate (i.e. at concentrations lower than the EC_{50}) as an estimate of E_{\max}/EC_{50} as previously discussed by Shou et al (2008).

(9)

$$AUCr = \frac{1}{1 + Slope \times [I_u]}$$

DDI risk assessment, as recommended by the final FDA guidance¹ was determined using R3 (equations 10 and 11).

(10)

$$R3 = \frac{1}{1 + \left[\frac{d \times E_{\max} \times 10 \times I_{\max,u}}{EC_{50} + 10 \times I_{\max,u}} \right]}$$

d is the scaling factor and assumed to be 1; $I_{\max,u}$ is the maximal unbound plasma concentration of the inducer.

Using the initial slope to estimate E_{\max}/EC_{50} :

(11)

$$R3 = \frac{1}{1 + Slope \times 10 \times [I_u]}$$

Results

Time- and Concentration-Dependent Increases in Fold induction of CYP mRNA and Activity

Time-dependent increases in fold induction of CYP isoforms following treatment with the prototypical CYP inducers omeprazole, phenobarbital, efavirenz, or rifampicin are summarized in Figures 1 (mRNA) and Figure 2 (activity). Concentration-dependent increases in CYP mRNA and activity, after 72 h incubation with inducers, are summarized in Figure 3.

Induction of CYP1A2

Omeprazole elicited robust increases in CYP1A2 mRNA (up to 33-fold in one laboratory) after 6 h incubation (Figure 1A), which increased in a time-dependent manner, up to ~16- to 72-fold, after 72 h. Maximal-fold induction of CYP1A2 mRNA by omeprazole occurred between 24 and 48 h. In contrast, activity (Figure 2A) achieved maximal fold induction between 48 and 72 h. Phenobarbital caused concentration-dependent increases (i.e. non-zero slope) in CYP1A2 mRNA (Figure 3A) and activity (Figure 3B), but the overall maximal fold induction was low (only ~2-fold, for both mRNA level and activity) and highly variable between labs. This weak but concentration-dependent induction of CYP1A2 by phenobarbital lacked time-dependence for mRNA (Figure 1A), with median fold-induction of 1.8 to 2.9 from 6 to 72 h (Table 1).

Phenobarbital-mediated increases in CYP1A2 activity, however, increased time-dependently to approximately to 3.3-fold (median) after 48 h, with minimal increase after 72 h (Figure 2A).

Induction of CYP2B6

Phenobarbital, rifampicin and efavirenz demonstrated time-dependent increases in CYP2B6 mRNA and activity, and consistent with CYP1A2, longer incubation times appeared to be

required to achieve maximum fold induction of activity (Figure 2B) compared to mRNA (Figure 1B). CYP2B6 mRNA achieved near maximal fold induction between 24 and 48 hr following phenobarbital or rifampicin treatment, whereas activity required at least 48 h. Although efavirenz demonstrated concentration-dependent increases in CYP2B6 mRNA and activity, a marked decrease in fold induction was observed at the two highest concentrations tested (Figure 3C and D; characterized as a “bell-shaped” curve), which was likely due to cytotoxicity. Overall, both rifampicin and efavirenz-mediated induction of CYP2B6 demonstrated less time-dependence than phenobarbital, in particular with minimal additional increases in mRNA observed after 12 to 72 h incubation compared to 6 h (Figure 1B).

Induction of CYP2C Isoforms

Phenobarbital and rifampicin elicited weak, but concentration-dependent increases in CYP2C8, CYP2C9, and CYP2C19 mRNA (Figure 3A, and 3E) and of these three isoforms, CYP2C8 appeared to be the most sensitive to induction with up to, on average, ~8-fold induction by phenobarbital and ~5-fold induction by rifampicin after 72 h incubation (note that CYP2C activity was not determined). Although fold induction of CYP2C8 appeared to increase up to 24 h, further time-dependent increases in mRNA were not as clear between 24 and 48 h for both inducers (Figure 1C). Overall induction of CYP2C isoforms by efavirenz was low, with no concentration-dependent (i.e. significant non-zero slope/correlation) increases observed for CYP2C19 or CYP2C9. In contrast, efavirenz caused concentration-dependent increases in CYP2C8 mRNA (up to an average of 3-fold at 10 μ M), and while the average fold induction increased between 6 and 12 h, there was weak trend for increasing fold induction between 24 and 48h. In addition, at the highest concentrations tested (20 and 30 μ M), efavirenz elicited

decreases in the mRNA for all CYP2C isoforms investigated, similar to what was observed for CYP2B6.

Induction of CYP3A4

Rifampicin elicited a time-dependent increase in CYP3A4 mRNA (Figure 1F) and maximal-fold induction appeared to occur after 24 h, with no marked increases in mRNA after additional incubation time (48 or 72 h) in 6/7 laboratories. Efavirenz also displayed time-dependent induction of CYP3A4 mRNA (Figure 1F), with most laboratories achieving near maximal induction between 12 and 24 h and minimal increase after 48 or 72 h. As was observed with CYP1A2 and CYP2B6, additional time was required to achieve maximal induction of CYP3A4 activity, with both rifampicin and efavirenz requiring at least 48 h (Figure 2C). Both inducers demonstrated clear concentration-dependence of both mRNA (Figure 3C and Figure 3E) and activity (Figure 3D and Figure 3F), but the two highest concentrations of efavirenz (20 and 30 μ M) caused marked decreases in CYP3A4 mRNA and activity (compared to the response at 10 μ M), resulting in “bell-shaped” curves consistent with the similar decreases observed for CYP2B and CYP2C isoforms. In contrast, rifampicin did not elicit decreases in fold induction of mRNA or activity at the higher concentrations tested.

Effect of Incubation Time on Estimates of Induction Parameters E_{\max} and EC_{50}

The fold induction following treatment of human hepatocytes with the full concentration range (8 concentrations) of each inducer was determined at 6, 12, 24, 48, and 72 h, which enabled estimation of the E_{\max} and EC_{50} at each time point (Table 1). Box and whisker plots summarizing the estimated E_{\max} and EC_{50} values for all inducers and CYP isoforms are also shown in

supplementary figures 1 and 2. In general, the model estimated values for E_{\max} demonstrated similar trends to the maximum observed fold induction. Notably, E_{\max} based on activity required longer incubation times to reach maximum than those from mRNA. Qualitatively, phenobarbital, efavirenz, and rifampicin achieved maximum E_{\max} values for CYP2B6 and CYP3A4 mRNA after 24 h, with minimal additional increase in the median E_{\max} values with increasing incubation time up to 72 h. In contrast, omeprazole-mediated induction of CYP1A2 required additional time to reach maximal response; at 12 h the maximum E_{\max} was only ~20-fold, compared to 60- to 100-fold at 24 to 72 h. E_{\max} estimates based on activity displayed a greater time-dependence than estimates based on mRNA, and most inducers required at least 48 h to achieve maximum fold induction. In addition, overall variability in maximal activity response across laboratories was less compared to mRNA, which is likely due to the higher degree of donor variability in the basal expression of CYP mRNA, and the higher dynamic range to detect small changes in mRNA compared to determination of CYP activity by probe substrate turnover.

In contrast to E_{\max} , estimates of potency (EC_{50}) were insensitive to incubation time with no clear trend to increase or decrease with time (Supplementary Figure 2). However, variability in potency was observed, which varied as much as 10- or 100-fold across laboratories (i.e. individual donors, since each lab used a different donor), and unlike estimates of E_{\max} , this variability was not higher after earlier incubation times compared to later ones. Based on previous work by the IWG, this variability in induction response is likely not due to differences in experimental procedure but intrinsic differences in induction response by the different hepatocyte donors (Kenny et al., 2018). In addition this up to two orders of magnitude variability observed in EC_{50} across the 7 participating laboratories is consistent with a previous IWG

publication indicating 130-fold range in EC₅₀ (rifampicin-3A4) based on data from 38 donors and 9 different participating laboratories (Supplemental Table 3, Kenny et al., 2018).

Sensitivity to Induction at Different Time Points

To further examine the relationship between incubation time and induction, the % of hepatocyte donor lots demonstrating a positive response (defined as a maximal fold induction > 2-fold) at 6, 12, 24, 48, or 72 h after treatment with prototypical inducers is summarized in Table 2.

Rifampicin required the shortest incubation time to elicit positive responses, with 100% of hepatocyte donors displaying >2-fold induction of CYP3A4 mRNA after 6 h incubation. CYP1A2 mRNA appeared to be the least sensitive to induction, with only 40 to 67% of donors achieving >2-fold induction after a 6-hour incubation with omeprazole or phenobarbital. As expected, activity-based determination of E_{max} at early time points was less sensitive than mRNA, and after 6 h none of the hepatocyte donors achieved >2-fold induction of CYP3A4 or CYP2B6 activity following treatment with rifampicin or efavirenz, respectively. The minimum incubation time required to achieve 100% positive induction response for CYP1A2, CYP2B6, and CYP3A4 activity with omeprazole, phenobarbital, or rifampicin, respectively, was 24 h. In addition, it was of interest to determine the % of hepatocyte donors achieving > 10-fold induction after incubations of 6 to 72 hours, and these values are included in the last row of Table 2. After 6 h incubation, only 20% of the donors achieved > 10-fold induction of CYP3A4 mRNA, and incubations > 12 hours were required to achieve this level of induction in > 80% of donors.

Comparison of the Average Fold Error (AFE) of E_{max}, EC₅₀ and E_{max} / EC₅₀ Estimates Relative to 72 h

Similar to previous reports (Kenny et al., 2018), large variability in induction response was observed between individual hepatocyte donors, complicating comparison of E_{\max} and EC_{50} estimates across time points. Therefore, to summarize the relationship between induction response and time across laboratories a paired approach was used, where estimates of E_{\max} and EC_{50} generated within the same laboratory were compared and then aggregated across companies, isoforms and/or compounds. Average fold error (AFE) was determined for induction parameter estimates measured at earlier time points (6, 12, 24, or 48 h) compared to estimates determined at 72 h; individual fold error was determined for each specific inducer – isoform paired with data from the same laboratory. AFE and % within 2-fold of E_{\max} , EC_{50} , or E_{\max}/EC_{50} estimates at 6, 12, 24 or 48 h compared to 72 h are summarized in Figure 4 and Table 3. Acceptable agreement between earlier time points and 72 h was defined as AFE between 0.5 and 2.0, representing a 2-fold under or over prediction, respectively. At 48 h, all three parameters (E_{\max} , EC_{50} , and E_{\max}/EC_{50}) agreed with estimates at 72 h, with AFE ranging from 0.79 to 1.1, indicating that incubations at 48 h and 72 h provided consistent induction responses with respect to maximal induction response and potency. In addition, > 88% of E_{\max} estimates (based on both mRNA and activity) determined at 48 h were within 2-fold of estimates at 72 h, further supporting good agreement between 48 and 72 h endpoints.

In general, E_{\max} determined at earlier time points based on mRNA demonstrated greater agreement with 72 hr determinations than E_{\max} estimates based on activity. After 12- or 24-hour incubations, mRNA-based estimates were still within 2-fold of estimates determined at 72 h (AFE = 0.58 and 0.74, respectively), whereas estimates based on activity were approximately 2- to 3- fold under predictive of the 72 h values, with AFE = of 0.50 and 0.27 respectively. In addition, the number of laboratories reporting measurable CYP activity at 6 h and 12 h was

notably lower than for incubations of 24 to 72 h, suggesting these short incubations may not be suitable for induction assessment. In contrast, at 24 to 72 h, the majority of laboratories reported mRNA and activity values for the AFE calculation, increasing confidence in the two-fold agreement observed.

Estimates of potency (EC_{50}) were relatively consistent (but still within 2-fold) across time points, with the AFE values ranging from 1.1 to 1.3 (mRNA) or 0.73 to 1.9 (activity) over the incubation times investigated. In addition, considerable variability in the AFE was observed for EC_{50} values, with 42 to 70% (mRNA) or 21 to 44% (activity) falling within 2-fold.

Comparison across time points for specific CYP isoforms

To determine if the relationship between parameter estimates and time was consistent across different CYP isoforms, the AFE for individual CYP isoforms was calculated and also included (in addition to the overall values) in Table 3. Overall, the AFE values for the individual CYP isoform-inducer pairs were similar to the overall AFE calculated for all isoforms comparing 6, 12, 24, or 48 h with 72 h. However, one notable exception was at 6 h, where E_{max} values for CYP1A2 and CYP2B6 activities at 6 h underpredicted values at 72 h by 10-fold (AFE=0.10), compared to a 4.5-fold underprediction for CYP3A4 (AFE=0.22). This discrepancy in AFE for different CYP isoforms was not apparent at later time points (48 and 72 h), where the AFE values for CYP1A2, 2B6, and 3A4 isoforms were relatively consistent, with good agreement (within 2-fold) for all three parameters investigated. Interestingly, at 48 h, CYP1A2 (activity, E_{max}) exhibited an AFE of 0.81 compared to AFE's of 0.90 for CYP2B6, and CYP3A4, suggesting that CYP1A2 activity may continue to increase after incubations longer than 72 h.

With respect to assessments determined at earlier time points, E_{max} estimates based on mRNA for all isoforms exhibited improved agreement than estimates based on activity. CYP2B6, in

particular, had 5- to 10-fold under-prediction of 72 h- E_{\max} based on activity at 6 and 12 h (AFE of 0.21 to 0.10); in contrast E_{\max} based on mRNA was under-predicted by 1.7- to 2.3-fold.

Comparison of CYP3A Drug-Drug Interaction Risk Assessment with Respect to Time

To explore the relationship between incubation duration and DDI risk assessment, the magnitude of a rifampicin-mediated in vivo drug-drug interaction (i.e., the change in victim exposure, AUCr, calculated using equation 7) was predicted for CYP3A using the E_{\max} and EC_{50} estimates at 6, 12, 24, 48, or 72 h (Figure 5A and Figure 5B, for mRNA and activity, respectively). The corresponding AFE for AUCr determined at 6, 12, 24 or 48 compared to 72 h is shown in Figure 5C and Figure 5D. It should be noted that since the magnitude of induction-mediated DDI increases with decreasing AUCr, AFE values > 1.0 represent underpredictions, unlike for E_{\max} where AFE > 1.0 represent over-predictions. As was observed for the individual E_{\max} and EC_{50} estimates, there was good agreement for the predicted AUCr between 48 and 72 h (AFE = 0.92 and 1.3, for mRNA and activity, respectively). AUCr determined at 48 h in 7/7 labs (100%) was within 2-fold of the AUCr determined at 72 h, based on mRNA, and for activity it was 85%, further supporting the use of 48 h incubations. Predicted AUCr based on mRNA remained acceptable after 12- or 24-hour incubations (AFE = 1.5 or 0.92, respectively) but risk assessment using activity tended to underpredict at these earlier time points by 3.8-fold (12 h) and 2.1-fold (24 h). In addition, AUCr determined at 24 hr by 6/7 laboratories (86%) based on mRNA was within 2-fold of AUCr determined at 72 hr, further emphasizing the utility of this shorter incubation for DDI risk assessment. While encouraging for rifampicin-CYP3A4 induction, the use of 24 h incubations for induction risk assessment should be considered carefully, since across all isoforms and inducers investigated, 68% of mRNA-based determinations of E_{\max} were within

2-fold of determinations from 72 h. Additional work is required to further validate the use of 24 h incubations for quantitative induction DDI risk assessment, in particular for non CYP3A4 isoforms.

Guidelines on Model Fitting Fold Induction Data

Initial attempts to collate the large volume of induction time-course data generated by 7 IWG laboratories revealed inconsistencies in the approach toward the curve fitting of fold induction data. Individual labs had independently developed separate ‘best practices’ around several key criteria, such as the choice of non-linear regression model and suitable acceptance criteria for parameter estimates. In addition, different strategies were implemented to address incomplete concentration-response curves, where the fold induction over the concentration range tested was insufficient to define E_{\max} . Fitting nonlinear models to incomplete curves has been shown to generate biased and/or imprecise estimates (Dutta et al., 1996; Schoemaker et al., 1998; Kirby et al., 2011). Further, correlated parameter estimates (such as E_{\max} and EC_{50}) complicate simple comparisons and have design implications (Sebaugh, 2011). Discriminating between (non)linear models is challenging in particular for standard induction experimental designs like those evaluated here (see Spiess and Neumeyer (2010) for a critique of R^2 in the nonlinear setting, Kirby et al (2011) and Brewer (2016) for the use of information theoretic measures in a linear regression setting). Kenakin (2009) suggests constraining one or more parameter estimates, if necessary, and suggests that the difference between the observed and estimated E_{\max} be less than 25%.

Recognizing the need for consistent data processing and analysis for the present time-course analysis the large induction data set was reviewed with the following objectives in mind: 1) establish criteria for excluding data points for atypical dose-response curves 2) recommend strategies to address incomplete (E_{\max} not achieved) dose-response curves and risk assessment for DDI and 3) determine the optimum model(s) for non-linear regression and estimation of induction parameters.

Intra-Sample Assay Variability

During the initial data review, the % CV was calculated for each set of triplicates. Despite varying a large number of conditions (e.g., donor, company, concentration, etc.) the average or median fold induction % CV appeared comparable across time, inducers and isoforms (Supplemental Figure 3). Considering the large range of measured fold inductions this suggested the intra-sample variance was proportional to the average, a common feature of in vitro assays. The average % CV differed between mRNA and activity, a potential intrinsic distinction between the two assays. For our analyses, these data suggested the use of a combined variability estimate. USP <1032> recommends the use of a robust pooled variance estimate when confronted with a need to identify, for example, ‘outliers’. Since the majority of the %CV for mRNA and activity was below 30%, an approximate average acceptable % CV for triplicate determinations for the present studies was set to 30%. Individual laboratories are encouraged to establish their own historical estimates. Now, if a known intra-sample variance is assumed, then a large sample two-sided confidence interval for the true fold induction mean is $\bar{x} \pm z_{\alpha/2} \sigma/\sqrt{n}$. For the largest observed average fold induction based on a set of triplicates, and a proxy for E_{\max} , replacing σ with its estimate %CV $\times \bar{x}$ and dividing the resulting interval by the observed average yields $1 \pm z_{\alpha/2} \times 0.30/\sqrt{3}$. As an approximate illustration, for $\alpha=0.10$ the right-hand portion simplifies to

± 0.28 . Subject to the precise choice of α and $z_{\alpha/2}$ vs $t_{\alpha/2}(\text{df})$, where the degrees of freedom can be specified by the design, in addition to refining the %CV estimate, an approximate range of plausible average fold inductions, consistent with the observed maximum fold induction, can be calculated. While we do not claim these intervals have optimal or desirable coverage properties, such an interval allows experimentalists to define a range of values consistent with the largest observed fold induction.

Special Considerations: “Bell-Shaped” and Incomplete Dose-Response Curves with Poorly Defined Maximum Fold Induction

Typical fold induction vs concentration plots resemble classical sigmoidal dose-response curves (Figure 6A, rifampicin). Importantly, fold induction is assumed to approximately plateau at high concentrations using conventional empirical models. Assuming a constant average at high concentration, while incorrect, is preferred to a decreasing non-monotonic relationship. In contrast, experimentalists can be confronted with “bell-shaped” curves, characterized by a decrease in fold induction at concentrations higher than the observed maximum fold induction concentration, creating a “bell” shape (Figure 6B, efavirenz). The paradoxical decrease at high test article concentrations is usually due to cytotoxicity, and assays confirming this loss in hepatocyte viability can provide definitive evidence to exclude these data points from curve-fitting and analysis. However, cytotoxic endpoints are typically indicative of near terminal cell death and may not provide enough resolution to identify scenarios where non-selective cellular injury obscures CYP induction of mRNA or activity. In addition, reduced fold induction could be due to downregulation of CYP (Hariparsad et al., 2017), or other complex or secondary pharmacology effects may be present. Therefore, cytotoxicity, as determined by standard assay endpoints, may not be detected at higher test article concentrations where the fold induction

decreases. Incorporating data where fold induction decreases at higher concentrations into the curve fit, in the absence of the use of a robust or weighting strategy to mitigate their effect, can bias the resulting nonlinear estimates, e.g., underestimate E_{\max} .

To establish a rationale for excluding (decreasing) fold induction data at higher concentrations without accompanying cytotoxicity data prior to curve fitting, the previously stated two-sided confidence interval are used to establish a range of acceptable fold induction above or below the highest observed fold induction.

Table 4 summarizes the several two-sided confidence intervals (0.8 to 0.975) and %CV (10 to 30%) for a plausible lowest and highest fold induction range assuming an observed fold induction of 100. For example, assuming an overall %CV of 30% and a two-sided 90% confidence interval, a 30% decrease in fold induction is plausible given sampling variability and the statistical precision of the observed ‘average’ E_{\max} . Here, it is assumed that the observed E_{\max} is representative of the actual unobserved E_{\max} and that the potential for bias is acceptable. In this example, concentrations yielding a decrease in fold-induction above that associated with the observed E_{\max} are removed from the analysis when the fold induction is < 70% of the observed E_{\max} . This approach provides a potentially conservative criterion to exclude data from curve fitting based on a given confidence level and expected variability (%CV). Individual labs are therefore advised to establish their own expectations around variability and a suitable confidence interval when setting criteria to exclude points and adequately model non-monotonic data. Removing data at higher concentrations using this approach typically results in an incomplete curve where the plateau (E_{\max}) is not adequately described, and strategies to address this scenario are reviewed below.

In addition to bell-shaped curves, atypical or incomplete fold induction vs concentration response curves may also arise when an apparent plateau of maximal induction response is not achieved, resulting in poor estimates of E_{\max} . Failure to observe consistent maximal fold induction at high concentrations could be due to cytotoxicity or solubility limitations. Using the same confidence interval for the largest observed fold induction, E_{\max} estimates that are appreciably larger than the observed maximum fold induction should be interpreted with caution or rejected. Confidence intervals/standard error estimates for E_{\max} from nonlinear regression models can be highly variable for small samples, especially when E_{\max} is not achieved. As described above, based on a two-sided 90% confidence interval and a CV of 30%, E_{\max} values greater than 130 should be treated with suspicion. Although unintentional, this recommendation agrees with the suggested guidelines from Kenakin (2009).

Comparison of Non-linear Regression Models For Estimation of E_{\max} and EC_{50} from Fold Induction Data Estimation of E_{\max} and EC_{50} for rifampicin or efavirenz by fitting fold-induction data generated by a single laboratory to 5 commonly used non-linear regression models is summarized in Table 5. The rifampicin concentration range tested (0 to 20 μM) displayed a classical sigmoidal concentration-response curve with well-defined minimum and maximum-fold induction, and all 5 models yielded similar estimates of E_{\max} and EC_{50} . Review of the AICc weights for each model fit indicated that the logistic 4P model had the highest probability of being the best fitting model (0.94) whereas all other models had very low probabilities (0.00497 to 0.0286). Remarkably, despite this large difference in AICc weight the induction parameter estimates were very similar for all 5 models (17.7 to 19.5 for E_{\max} and 0.287 to 0.340 μM for EC_{50}). Therefore, assessment of the probability of the best-fitting model for fitting fold induction

data using Akaike information criterion has minimal impact on the estimation of E_{\max} and EC_{50} , for induction curves that define the maximum fold induction. In addition, since all 5 models provided consistent estimates of E_{\max} and EC_{50} , risk assessment for induction-mediated DDI is also unaffected by the choice of model for fitting, for curves resembling this rifampicin dose-response.

To further investigate the effect of model selection on induction parameter estimates for other CYP inducer and CYP isoforms, fold induction data determined by each laboratory were used to fit the 5 models and the E_{\max} and EC_{50} values were compared (Supplementary Figure 4).

The absolute average fold error (AAFE) determined for each model's estimate of E_{\max} and EC_{50} was compared to the best model's estimate, determined by AICc weight. Overall, as was observed for rifampicin and CYP3A4, all 5 model fits produced similar estimates of E_{\max} , with > 80% of the model fits for all models within $\pm 20\%$ (AAFE = 1.2) of the best model fit (Supplemental Figure 4A). Estimates of EC_{50} also showed good agreement across all models with > 75% between ± 20 and 50% of the best model estimate (Supplemental Figure 4B; AAFE = 1.2 to 1.5). Therefore, as observed for rifampicin-3A4, model selection overall for all isoforms and inducers investigated has little impact on the actual estimated induction parameters E_{\max} and EC_{50} for typical fold induction curves.

The effect of model selection on induction parameter estimates was also investigated for atypical dose-response curves (Table 5). In contrast to rifampicin, the 5 models provided different induction parameter estimates characterizing the fold induction of CYP3A4 mRNA by efavirenz, which displays a “bell-shaped” curve (Figure 6B). The two highest concentrations where the fold induction decreased more the 30% compared to the maximum fold induction were excluded from the analysis. Consequently, the remaining efavirenz concentrations did not elicit adequate fold

induction to define the E_{\max} (i.e., an atypical dose-response where E_{\max} is not achieved). Three of the models (logistic 3P, E_{\max} , and hyperbolic fits) estimated E_{\max} values that were > 2-fold higher than the observed maximal fold induction (15-fold), and were rejected based on the developed criteria (i.e. > 130% of observed E_{\max} ; with a maximum observed fold induction of 15, E_{\max} estimates > 19.5, or 130% of 15, would be rejected). Interestingly, comparison of AICc weight suggests the best model was the sigmoidal 3P fit (AIC weight = 0.70), and the next best fit was the logistic 4-parameter (AIC weight = 0.297); the estimated E_{\max} using these two models were within 130% of the observed maximum fold induction. In contrast, the logistic 3P, E_{\max} , and hyperbolic models all exhibited low probability of being the best model (AICc weight < 0.00327) and provided very high estimates of E_{\max} that were >2-fold higher than the observed maximum fold induction. Therefore, for this example of a curve with poorly defined E_{\max} , models with higher probability of being the best-fitting model as determined by AICc weight also provide E_{\max} estimates that are closer to the observed maximum fold induction.

Initial Slope as an Estimate of E_{\max}/EC_{50}

In cases where non-linear regression models fail to provide reliable induction parameter estimates the initial slope of the fold induction vs (linear) concentration plot can provide an estimation of E_{\max}/EC_{50} , under the assumptions suitable for such a simplified model (Shou et al., 2008). To investigate the utility of this approach, the initial slopes for all isoform-inducer pairs were calculated by linear regression of the fold induction vs (non-log) concentration at each time point, and the AFE of the slope compared to the actual E_{\max}/EC_{50} (determined at 48 h) is summarized in Figure 7. On average, the initial slope underpredicted the actual E_{\max}/EC_{50} by about 2-fold after 48 h incubation, with AFE of 0.45 (mRNA) and 0.63 (activity). Overall, initial slopes determined at early time points (6 to 24 h), based on mRNA or activity yielded poor

estimates of E_{\max}/EC_{50} ($AFE = 0.11$ to 0.29). In addition, this analysis was repeated (data not shown) by comparing initial slope to the E_{\max}/EC_{50} determined at 72 h, and the AFE was similar to that observed after 48 h incubation, with the initial slope (determined at 48 h) underpredicting by approximately 2-fold.

Effect of Model Fitting Approaches on Induction DDI Risk Assessment

Due to the consistency in the fitted E_{\max} and EC_{50} , DDI risk assessment for inducers displaying a typical sigmoidal dose-response (with well-defined maximum fold induction) would be similar regardless of the model fitting approach. However, for incomplete dose-response curves (such as efavirenz) with poorly defined maximal fold induction, DDI risk assessment would likely be dependent on the model selected to estimate E_{\max} and EC_{50} . To further explore the relationship between the selection of model to fit induction data and DDI risk assessment for an atypical dose-response curve, Table 6 summarizes the model estimates for E_{\max} , EC_{50} and the corresponding F2 and R3 (equation 10) using the logistic 3P, sigmoidal 3P, or a constrained logistic 3P fit, for efavirenz-mediated induction of CYP3A4 mRNA. Note that this curve is also presented in Figure 6B. Based on our criteria, the estimated E_{\max} using the logistic 3P equation would be rejected since it is $> 130\%$ above the observed maximum-fold induction, but the induction risk assessment was included for comparison using this estimate. Using the logistic 3P equation to fit the data yielded a less conservative estimate of R3 (0.27) compared to the other approaches, which was mainly due to the decrease in potency ($EC_{50} = 16.5$) due to a much higher estimate of E_{\max} (38.5). This example highlights the corresponding right-shift (underestimation

of potency) in EC_{50} when over-estimating E_{max} . In addition, R3 appears to be more sensitive to EC_{50} than E_{max} in this example, since even though the logistic 3P estimated a >2-fold E_{max} than the other approaches, the overall predicted in vivo interaction was less, which was primarily driven by the decrease in potency (i.e. left-shift and increased EC_{50}). The next approach explored was to constrain the E_{max} to the observed maximum fold induction using the logistic 3P fit, which yielded an E_{max} of 15.1 and an EC_{50} of 3.1 μ M. These values were similar to the model estimates using the sigmoidal 3P fit (15.1 and 3.6 μ M, respectively), and the corresponding predicted reduction in a victim drug's exposure was similar for both approaches ($R3 = 0.19$ to 0.20).

Use of Initial Slope for Estimation of E_{max}/EC_{50} and DDI Risk Assessment

Despite a tendency to underpredict the E_{max}/EC_{50} by about 2-fold, the utility of using the initial slope to assess induction DDI risk for efavirenz was investigated (last row of Table 6). Using the initial linear slope of the fold induction vs concentration yielded an estimated E_{max}/EC_{50} of 1.5, and a corresponding predicted R3 (equation 11) of 0.35 which is an approximate 2-fold underprediction compared to assessment based on the sigmoidal-3P fit (0.19). Comparison of these two approaches to determine R3 was further investigated using data from all participating laboratories and the AFE's are summarized in Table 7 for omeprazole, efavirenz, and rifampicin. Interestingly, the R3 values determined using the initial slope estimation compared to the sigmoidal-3P fit exhibited good agreement (AFE = 0.955 and 0.823) for efavirenz-CYP2B6 and rifampicin-CYP3A4. Acceptable agreement (within 2-fold) was also observed for omeprazole-1A2 and efavirenz-3A4 (AFE = 0.685 for both). This agreement to estimate R3 despite a ~2-fold underprediction of E_{max}/EC_{50} using the initial slope is likely due to the conservative nature of the R3 equation which utilizes a 10x factor on the input unbound inducer concentration, which

effectively minimizes the underprediction of E_{\max}/EC_{50} . While preliminary, this limited data set indicates agreement (overall AFE=0.83) between the R3 estimated using the initial slope and the R3 value calculated using E_{\max} and EC_{50} determined using a sigmoidal 3P fit.

General Guidelines for Estimation of E_{\max} and EC_{50} from Fold Induction Data

A summary of the recommended approach towards model fitting fold induction data is presented in Figure 8.

Discussion

Regulatory agencies recommend assessment of induction-mediated DDI using primary human hepatocyte cultures for up to 72 h, which has been adopted in industry (Meunier et al., 2000; Chu et al., 2009). However, evaluating induction using shorter durations could be advantageous due to the potential for cytotoxicity after prolonged exposure to NCE's, and therefore shorter incubation times could enable induction DDI risk assessment that would otherwise not be possible. The objective of the present study was to compare the induction response, and corresponding DDI risk assessment, in primary human hepatocytes following treatment with 4 prototypical CYP inducers. This study was designed to systematically evaluate the time course of CYP induction using mRNA and enzyme activity endpoints. Importantly, the study was conducted by seven different laboratories, using independent hepatocyte donors, employing their own protocols.

Overall, maximal fold induction of mRNA occurred after shorter duration than that required for activity, which is consistent with literature reports. Li et al. (1997) and LeCluyse et al. (2000) previously demonstrated that CYP3A activity increases time-dependently up to 72 h, whereas maximal CYP3A4 mRNA levels have been observed after 18-24 h (Drocourt et al., 2001), and within 24 h for CYP1A2 (Grover et al., 2007). Zhang et al (2010) also reported that CYP1A2, 2B6, and 3A4 exhibited robust increases in mRNA after 6 h and achieved maximal induction of mRNA levels within 24 h. Faucette et al (2004) reported maximal induction of CYP3A4 (by rifampicin) within 2 to 4 days, whereas CYP2B6 activity continued to increase until 4 days of treatment. In the present study, average maximal fold induction of CYP1A2, CYP2B6, and CYP3A4 mRNA occurred after 24 to 48 h incubations (Figure 1A, B, and F), whereas 48 h was required to achieve maximal activity (Figure 2). Estimates of the E_{\max} followed the same trend,

with mRNA-based assessments determined at 24 and 48 h exhibiting good agreement with 72 h (AFE=0.74 and 0.94, respectively, Figure 4A), whereas assessments based on activity required at least 48 h to fall within 2-fold of 72 h.

The utility of earlier assessment of CYP induction based on mRNA was reported by Sane et al. (2016), with maximal induction occurring between 8 and 12 h and corresponding DDI risk assessment consistent with assessments at 48-72 h. Zhang et. al (2010) also concluded that 24 or 48 hour assessments based on mRNA are suitable for routine testing without sacrificing assay robustness. An additional factor supporting shorter durations for assessment of induction is the reported loss in enzyme activity in cultured primary hepatocytes resulting in lower basal CYP activity compared to freshly isolated hepatocytes (Hamilton et al., 2001; Rodriguez-Antona et al., 2002; Elaut et al., 2006). Hepatic dedifferentiation and the contribution of micro-RNA have been proposed drivers for this loss in activity (Bell et al., 2016; Lauschke et al., 2016), but the precise mechanism has yet to be determined. Nevertheless, these decreases in CYP activity in hepatocyte culture further support the use of shorter incubations to assess the risk for induction-mediated DDI.

The time to achieve maximum-fold induction can also be considered in context with respect to the reported degradation rates (k_{deg}) for CYP protein or mRNA. The time to maximum induction is analogous to achieving a new steady-state concentration and is therefore intrinsically related to the k_{deg} . Recent reports (Ramsden et al., 2015; Takahashi et al., 2017) using long term hepatocyte co-cultures have estimated k_{deg} for CYP3A4 protein to be $\sim 0.02 \text{ h}^{-1}$ ($T_{1/2} \sim 30 \text{ h}$) which is consistent with values determined in hepatocytes (Maurel, 1996; Yang et al., 2008) and liver slices (Renwick et al., 2000). A similar k_{deg} value has been reported for CYP3A4 mRNA

(Yamashita et al., 2013). In order to achieve “true” steady-state kinetics and a maximum fold induction, 5 half-lives (150 h) would be required – within 2-fold of the 3-day period reported by LeCluyse et al. (2000) and ~3-fold higher than our data (suggesting 48 h is sufficient). However, after a single half-life (~ 30 h), induction should be within 50% of steady-state, and after 2 half-lives it would be within 75%. Therefore, similar maximal-fold induction after 48 and 72 h is consistent with achieving between 50 and 75% of E_{\max} after 1.5 half-lives.

Previously, the IWG reported weak and variable induction of CYP2C8, CYP2C9, and CYP2C19 (Hariparsad et al., 2017). In the present study, phenobarbital and rifampicin elicited concentration-dependent increases in CYP2C9 and CYP2C19 mRNA, but the maximum fold induction was weak (< 2-fold; Figure 3C,E). Induction of CYP2C8 mRNA displayed minimal time-dependence, with near maximal induction occurring after 12 to 24 h, with minimal increases after 48 or 72 h (Figure 1D). These data suggest that longer incubation times are not required to achieve maximal fold induction of CYP mRNA, even for weak induction (i.e. CYP2C8). Therefore, conclusions around agreement between E_{\max} and EC_{50} estimates at 24 or 48 h and estimates after 72 h are likely applicable to both weak and strong inducers.

General Recommendations on Incubation Duration for Induction Risk Assessment and Model Fitting

1. 48-hour and 72-hour incubations in primary hepatocytes provide equivalent assessment of CYP induction, based on mRNA or CYP activity.

Across all donors, CYP isoforms, and inducers, E_{\max} and EC_{50} estimates demonstrated excellent agreement ($AFE > 0.87$) between 48 and 72 h incubations, based on both mRNA and activity. In

addition, 72 h incubations provided no improvement over 48 h for predicting the likelihood of a rifampicin-mediated DDI (AFE = 0.92 to 1.3). The IWG recommends incubations of 48 h for assessing the risk for induction-mediated DDI for CYP inducers using mRNA or activity as the endpoint.

2. Assessment of CYP induction after 24 h, based on mRNA, but not activity, provides reliable determination of induction parameter estimates and DDI risk.

Incubations for 24 h yielded mRNA-based induction estimates of E_{\max}/EC_{50} that were similar to 72 h (AFE=0.055, 1.8-fold underpredicted; Figure 4), whereas activity-based assessments underpredicted by 2.8-fold. Risk assessment for rifampicin-mediated DDI based on CYP3A4 mRNA determined after 24 h also exhibited good agreement with 72 h (AFE = 0.92, Figure 5A,C), with 6/7 laboratories (86%) predicting within 2-fold, supporting the utility of 24 h incubations. However, when considering the variability in mRNA response across all isoforms and inducers (68% of E_{\max} determinations were within 2-fold of 72 h), induction assessment after 24 h should be interpreted carefully, in particular for non-CYP3A4 interactions.

3. Compounds causing less than 2-fold induction of mRNA, and no concentration dependence, after 12 h can be classified as negative for CYP induction

Previously, IWG recommended that compounds demonstrating < 2-fold induction of CYP3A4 mRNA (48 or 72 h) and no evidence of concentration-response be classified as negative for induction when the corresponding rifampicin response in the same donor is ≥ 10 -fold (Kenny et al., 2018). In the present study 6/7 labs reported >10-fold CYP3A4 induction with rifampicin after 12 h, and all labs were > 10-fold for durations ≥ 24 h. Therefore, compounds demonstrating

<2-fold induction (and no concentration-dependent response) of mRNA after 12 or 24 h can be classified as negative for CYP3A4 induction.

4. Atypical concentration vs fold induction responses (i.e. ‘Bell-Shaped’ curves or failure to achieve E_{\max}) can be addressed by removing points outside an established confidence interval with an expected %CV.

With an expected estimate of variability (30% CV) and a two-sided confidence interval of 0.95, concentrations above that associated with the E_{\max} exhibiting a paradoxical decrease in fold induction are removed from induction curve fitting when the fold induction is < 70% of the observed E_{\max} . Similarly, estimates of E_{\max} that are > 130% of the observed maximum-fold induction are interpreted with caution, based on the same estimates of variability and assumed confidence interval. The estimate of 30% is based on the overall triplicate variability observed across all 7 labs participating in this study; investigators are encouraged to leverage their own estimates of variability to establish individual guidelines.

5. When the maximum and minimum fold induction are well defined by the concentration range tested, selection of the best fitting model using AICc criteria has little impact on the estimated E_{\max} and EC_{50}

For fold induction curves demonstrating classical sigmoidal kinetics, all 5 non-linear regression models provided similar estimates of E_{\max} and EC_{50} with > 75% falling within ± 20 to 50% of the best estimate as determined by the highest AICc weight. This consistency suggests that AICc criteria provides limited value to determine the best model with respect to the estimates of E_{\max} and EC_{50} and DDI risk assessment.

6. When the maximum-fold induction is not well defined, conservative estimates of E_{\max} and EC_{50} can be obtained using sigmoidal-3P fit or constraining logistic 3/4P fits to the maximum observed fold induction.

The sigmoidal 3P fit and constraining logistic 3- or 4-parameter fits to the maximum observed fold induction underestimates the E_{\max} and provide an over-estimation of potency (right-shifted EC_{50}). Therefore, sensitivity analysis assuming $E_{\max} >$ the fitted E_{\max} and $EC_{50} <$ the fitted EC_{50} using the constrained logistic 3P/4P or sigmoidal 3P fits provide a conservative approach to DDI risk assessment.

7. Preliminary data suggest initial slope of fold induction data may approximate E_{\max}/EC_{50} and enable DDI risk assessment in scenarios where E_{\max} and EC_{50} cannot be reliably estimated.

Importantly, the experimental design was not optimized to characterize the initial slope, and evaluation of induction response at concentrations below the EC_{50} would enable more accurate characterization. Recognizing these limitations, additional work is needed to further validate this approach for induction based DDI assessment, as it could provide a valuable approach when induction parameters cannot be derived experimentally. Encouragingly, preliminary analysis indicated the initial slope estimate of R3 for omeprazole, efavirenz or rifampicin was in good agreement ($AFE=0.83$) with R3 determined using E_{\max} and EC_{50} (using a sigmoidal-3P fit). Further investigation of this approach is ongoing.

The IWG has presented a data-driven evaluation of the time course for CYP induction by 4 prototypical inducers (omeprazole, phenobarbital, efavirenz, and rifampicin). Although there was

variability in induction response across different human hepatocyte donors and laboratories, consistent analysis using our model-fitting guidelines allowed several recommendations to be made regarding the appropriate incubation duration to obtain reliable induction parameter estimates. A key conclusion from this analysis is that 48 h incubations provide equivalent assessment of induction response and corresponding in vivo DDI risk assessment compared to 72 h incubations, indicating that longer incubations provide little benefit.

Acknowledgements

The authors would like to thank the IQ IWG for valuable discussion of data and manuscript review, the IQ TALG for manuscript review, the IQ member companies for data, Drs Ronald S. Obach (Pfizer), Christopher Gibson (Merck) and Michael Sinz (BMS) for valuable feedback on draft manuscripts. We would also like to thank the following individuals who contributed to in vitro (wet lab) induction studies presented in the manuscript: Stephanie Piekos (Boehringer Ingelheim), Carlo Sensenhauser (J&J), Amanda Moore and Hong Tsao (Vertex), Thuy Ho, Rob Clark and Sarah Trisdale (Corning Life Sciences), Xiaowei He (Eisai), Kelly Nulick (Pfizer).

Authorship Contributions

Participated in research design: Ramsden, Dallas, Einolf, Palamanda, Chen, Goosen, Siu, Zhang, Tweedie, Hariparsad, Jones

Performed data analysis: Wong, Yates, Fung, Ramsden, Goosen

Wrote or contributed to the writing of the manuscript: Wong, Ramsden, Dallas, Fung, Einolf, Chen, Goosen, Siu, Zhang, Tweedie, Hariparsad, Jones, and Yates

References

- Bell CC, Hendriks DF, Moro SM, Ellis E, Walsh J, Renblom A, Fredriksson Puigvert L, Dankers AC, Jacobs F, Snoeys J, Sison-Young RL, Jenkins RE, Nordling A, Mkrtchian S, Park BK, Kitteringham NR, Goldring CE, Lauschke VM, and Ingelman-Sundberg M (2016) Characterization of primary human hepatocyte spheroids as a model system for drug-induced liver injury, liver function and disease. *Sci Rep* **6**:25187.
- Brewer MJ, Butler, A., Cooksley, S.L (2016) The relative performance of AIC, AICC and BIC in the presence of unobserved heterogeneity. *Methods in Ecology and Evolution* **7**:679-692.
- Burnham KP and Anderson DR (2002) *Model Selection and Multimodel Inference*. Springer-Verlag, New York.
- Chu V, Einolf HJ, Evers R, Kumar G, Moore D, Ripp S, Silva J, Sinha V, Sinz M, and Skerjanec A (2009) In vitro and in vivo induction of cytochrome p450: a survey of the current practices and recommendations: a pharmaceutical research and manufacturers of america perspective. *Drug Metab Dispos* **37**:1339-1354.
- Drocourt L, Pascussi JM, Assenat E, Fabre JM, Maurel P, and Vilarem MJ (2001) Calcium channel modulators of the dihydropyridine family are human pregnane X receptor activators and inducers of CYP3A, CYP2B, and CYP2C in human hepatocytes. *Drug Metab Dispos* **29**:1325-1331.
- Dutta S, Matsumoto Y, and Ebling WF (1996) Is it possible to estimate the parameters of the sigmoid Emax model with truncated data typical of clinical studies? *J Pharm Sci* **85**:232-239.
- Elaut G, Henkens T, Papeleu P, Snykers S, Vinken M, Vanhaecke T, and Rogiers V (2006) Molecular mechanisms underlying the dedifferentiation process of isolated hepatocytes and their cultures. *Curr Drug Metab* **7**:629-660.
- Fahmi OA and Ripp SL (2010) Evaluation of models for predicting drug-drug interactions due to induction. *Expert Opin Drug Metab Toxicol* **6**:1399-1416.
- Faucette SR, Wang H, Hamilton GA, Jolley SL, Gilbert D, Lindley C, Yan B, Negishi M, and LeCluyse EL (2004) Regulation of CYP2B6 in primary human hepatocytes by prototypical inducers. *Drug Metab Dispos* **32**:348-358.
- Grover GS, Brayman TG, Voorman RL, and Ware JA (2007) Development of in vitro methods to predict induction of CYP1A2 and CYP3A4 in humans. *Assay Drug Dev Technol* **5**:793-804.

- Hamilton GA, Jolley SL, Gilbert D, Coon DJ, Barros S, and LeCluyse EL (2001) Regulation of cell morphology and cytochrome P450 expression in human hepatocytes by extracellular matrix and cell-cell interactions. *Cell Tissue Res* **306**:85-99.
- Hariparsad N, Ramsden D, Palamanda J, Dekeyser JG, Fahmi OA, Kenny JR, Einolf H, Mohutsky M, Pardon M, Siu AY, Chen L, Sinz M, Jones B, Walsky R, Dallas S, Balani SK, Zhang G, Buckley D, and Tweedie D (2017) Considerations from the IQ Induction Working Group in Response to Drug-Drug Interaction Guidances from Regulatory Agencies: Focus on Down-regulation, CYP2C Induction and CYP2B6 Positive Control. *Drug Metab Dispos*.
- Hewitt NJ, de Kanter R, and LeCluyse E (2007) Induction of drug metabolizing enzymes: a survey of in vitro methodologies and interpretations used in the pharmaceutical industry--do they comply with FDA recommendations? *Chem Biol Interact* **168**:51-65.
- Kenakin T (2009) *A Pharmacology Primer: Theory, Applications, and Methods 3rd Ed*. Elsevier Academic Press.
- Kenny JR, Ramsden D, Buckley DB, Dallas S, Fung C, Mohutsky M, Einolf HJ, Chen L, Dekeyser JG, Fitzgerald M, Goosen TC, Siu YA, Walsky RL, Zhang G, Tweedie D, and Hariparsad N (2018) Considerations from the Innovation and Quality Induction Working Group in Response to Drug-Drug Interaction Guidances from Regulatory Agencies: Focus on CYP3A4 mRNA In Vitro Response Thresholds, Variability, and Clinical Relevance. *Drug Metab Dispos* **46**:1285-1303.
- Kirby S, Brain P, and Jones B (2011) Fitting E(max) models to clinical trial dose-response data. *Pharm Stat* **10**:143-149.
- Laio F, Allamano, P., Claps, P. (2010) Exploiting the information content of hydrological "outliers" for goodness-of-fit testing. *Hydrol Earth Syst Sci* **14**:1909-1917.
- Lauschke VM, Vorrink SU, Moro SM, Rezayee F, Nordling A, Hendriks DF, Bell CC, Sison-Young R, Park BK, Goldring CE, Ellis E, Johansson I, Mkrtchian S, Andersson TB, and Ingelman-Sundberg M (2016) Massive rearrangements of cellular MicroRNA signatures are key drivers of hepatocyte dedifferentiation. *Hepatology* **64**:1743-1756.
- LeCluyse E, Madan A, Hamilton G, Carroll K, DeHaan R, and Parkinson A (2000) Expression and regulation of cytochrome P450 enzymes in primary cultures of human hepatocytes. *J Biochem Mol Toxicol* **14**:177-188.

- Li AP, Reith MK, Rasmussen A, Gorski JC, Hall SD, Xu L, Kaminski DL, and Cheng LK (1997) Primary human hepatocytes as a tool for the evaluation of structure-activity relationship in cytochrome P450 induction potential of xenobiotics: evaluation of rifampin, rifapentine and rifabutin. *Chem Biol Interact* **107**:17-30.
- Maurel P (1996) The use of adult human hepatocytes in primary culture and other in vitro systems to investigate drug metabolism in man. *Adv Drug Deliv Rev* **22**:105-132.
- Meunier V, Bourrie M, Julian B, Marti E, Guillou F, Berger Y, and Fabre G (2000) Expression and induction of CYP1A1/1A2, CYP2A6 and CYP3A4 in primary cultures of human hepatocytes: a 10-year follow-up. *Xenobiotica* **30**:589-607.
- Ramsden D, Fung C, Hariparsad N, Kenny JR, Mohutsky MA, Parrott N, Robertson S, and Tweedie DJ (2019) Perspectives from the IQ Induction Working Group on Factors Impacting Clinical DDI Due to Induction: Focus on CYP3A Substrates. *Drug Metab Dispos*.
- Ramsden D, Zhou J, and Tweedie DJ (2015) Determination of a Degradation Constant for CYP3A4 by Direct Suppression of mRNA in a Novel Human Hepatocyte Model, HepatoPac. *Drug Metab Dispos* **43**:1307-1315.
- Renwick AB, Watts PS, Edwards RJ, Barton PT, Guyonnet I, Price RJ, Tredger JM, Pelkonen O, Boobis AR, and Lake BG (2000) Differential maintenance of cytochrome P450 enzymes in cultured precision-cut human liver slices. *Drug Metab Dispos* **28**:1202-1209.
- Rodriguez-Antona C, Donato MT, Boobis A, Edwards RJ, Watts PS, Castell JV, and Gomez-Lechon MJ (2002) Cytochrome P450 expression in human hepatocytes and hepatoma cell lines: molecular mechanisms that determine lower expression in cultured cells. *Xenobiotica* **32**:505-520.
- Sane RS, Ramsden D, Sabo JP, Cooper C, Rowland L, Ting N, Whitcher-Johnstone A, and Tweedie DJ (2016) Contribution of Major Metabolites toward Complex Drug-Drug Interactions of Deleobuvir: In Vitro Predictions and In Vivo Outcomes. *Drug Metab Dispos* **44**:466-475.
- Schoemaker RC, van Gerven JM, and Cohen AF (1998) Estimating potency for the Emax-model without attaining maximal effects. *J Pharmacokinet Biopharm* **26**:581-593.
- Sebaugh JL (2011) Guidelines for accurate EC50/IC50 estimation. *Pharm Stat* **10**:128-134.
- Shou M, Hayashi M, Pan Y, Xu Y, Morrissey K, Xu L, and Skiles GL (2008) Modeling, prediction, and in vitro in vivo correlation of CYP3A4 induction. *Drug Metab Dispos* **36**:2355-2370.

- Spiess AN and Neumeyer N (2010) An evaluation of R² as an inadequate measure for nonlinear models in pharmacological and biochemical research: a Monte Carlo approach. *BMC Pharmacol* **10**:6.
- Sun Y, Chothe PP, Sager JE, Tsao H, Moore A, Laitinen L, and Hariparsad N (2017) Quantitative Prediction of CYP3A4 Induction: Impact of Measured, Free, and Intracellular Perpetrator Concentrations from Human Hepatocyte Induction Studies on Drug-Drug Interaction Predictions. *Drug Metab Dispos* **45**:692-705.
- Takahashi RH, Shahidi-Latham SK, Wong S, and Chang JH (2017) Applying Stable Isotope Labeled Amino Acids in Micropatterned Hepatocyte Coculture to Directly Determine the Degradation Rate Constant for CYP3A4. *Drug Metab Dispos* **45**:581-585.
- Wagenmakers EJ and Farrell S (2004) AIC model selection using Akaike weights. *Psychon Bull Rev* **11**:192-196.
- Yamashita F, Sasa Y, Yoshida S, Hisaka A, Asai Y, Kitano H, Hashida M, and Suzuki H (2013) Modeling of rifampicin-induced CYP3A4 activation dynamics for the prediction of clinical drug-drug interactions from in vitro data. *PLoS One* **8**:e70330.
- Yang J, Liao M, Shou M, Jamei M, Yeo KR, Tucker GT, and Rostami-Hodjegan A (2008) Cytochrome p450 turnover: regulation of synthesis and degradation, methods for determining rates, and implications for the prediction of drug interactions. *Curr Drug Metab* **9**:384-394.
- Yates P, Eng H, Di L, and Obach RS (2012) Statistical methods for analysis of time-dependent inhibition of cytochrome p450 enzymes. *Drug Metab Dispos* **40**:2289-2296.
- Zhang JG, Ho T, Callendrello AL, Clark RJ, Santone EA, Kinsman S, Xiao D, Fox LG, Einolf HJ, and Stresser DM (2014) Evaluation of calibration curve-based approaches to predict clinical inducers and noninducers of CYP3A4 with plated human hepatocytes. *Drug Metab Dispos* **42**:1379-1391.
- Zhang JG, Ho T, Callendrello AL, Crespi CL, and Stresser DM (2010) A multi-endpoint evaluation of cytochrome P450 1A2, 2B6 and 3A4 induction response in human hepatocyte cultures after treatment with beta-naphthoflavone, phenobarbital and rifampicin. *Drug Metab Lett* **4**:185-194.

Footnotes

¹ In Vitro Drug Interaction Studies – Cytochrome P450 Enzyme- and Transporter- Mediated Drug Interaction Guidance for Industry (Final Guidance, January 2020).

<https://www.fda.gov/regulatory-information/search-fda-guidance-documents/vitro-drug-interaction-studies-cytochrome-p450-enzyme-and-transporter-mediated-drug-interactions>

² Guidance on the investigation of drug interactions (EMA, June 2012).

https://www.ema.europa.eu/en/documents/scientific-guideline/guideline-investigation-drug-interactions_en.pdf

³ Pharmaceutical and Medical Devices Agency (PMDA) 2014 guidance [Drug Interaction Guideline for Drug Development and Labeling Recommendations (The Japanese Ministry of Health, Labour, and Welfare MHLW), updated 2017, English translation not yet available]

FIGURE LEGENDS

Figure 1: Summary of fold induction of CYP1A2, CYP2B6, CYP2C8, CYP2C9, CYP2C19, or CYP3A4 mRNA following treatment of human hepatocytes with omeprazole (100 μ M), phenobarbital (3000 μ M), efavirenz (30 μ M), or rifampicin (20 μ M) for 6, 12, 24, or 72 h. Each circle represents the mean fold induction from a single laboratory (i.e triplicate determination from a single experiment).

Figure 2: Summary of fold induction of CYP1A2, CYP2B6, or CYP3A4 activity following treatment of human hepatocytes with omeprazole (100 μ M) , phenobarbital (3000 μ M), efavirenz(30 μ M), or rifampicin (20 μ M) for 6, 12, 24, or 72 h. Each bar represents the mean of 7 labs with standard deviation.

Figure 3: Summary of concentration-dependent increases in fold induction of mRNA (CYP1A2, CYP2B6, CYP2C8, CYP2C9, CYP2C19, or CYP3A4) or activity (CYP1A2, CYP2B6, or CYP3A4) following treatment of human hepatocytes with phenobarbital, efavirenz, or rifampicin for 72 hours.

Figure 4: Comparison of overall fold error of parameter estimates E_{\max} (A), EC_{50} (B) or E_{\max}/EC_{50} (C) determined at 6, 12, 24, or 48 hours compared to the corresponding parameters determined at 72 hours. AFE was calculated for all inducers (omeprazole, phenobarbital, efavirenz, or rifampicin) and CYP isoforms (CYP1A2, CYP2B6 or CYP3A4) across all hepatocyte donors in a paired analysis, where parameters generated at the same laboratory were compared.

Figure 5: Comparison of predicted CYP3A in vivo DDI (AUCr) after rifampicin treatment based on mRNA (A) or activity (B) at 6, 12, 24, 48 or 72 hours. Corresponding average fold error

(AFE) between AUCr determined at 6, 12, 24, or 48 hours compared to 72 hours is summarized in for mRNA (C) or activity (D). Note that there was insufficient induction of CYP3A activity after 6 h to determine E_{\max} , EC_{50} and calculate AUCr.

Figure 6: Comparison of non-linear regression model fitting for A) rifampicin or B) efavirenz (“Bell shaped” Curve) induction of CYP3A4 mRNA. Shaded grey circles indicate data points removed from curve fitting based on an 30% CV and a two-sided 95% confidence interval. These concentrations, above that associated with the observed E_{\max} , exhibit fold induction that is < 70% of the observed E_{\max} (i.e. < 30% decrease).

Figure 7: Comparison of fold error of initial slope at 6, 12, 24, 48, or 72 hours compared to the E_{\max}/EC_{50} determined at 72 hours.

Figure 8: Recommend guidelines for model fitting fold induction data.

¹Assessment of Non-Zero Slope: Standard linear regression or Spearman’s nonparametric rank correlation coefficient used to confirm concentration dependence with non-zero slope or positive correlation.

²Exclude data points (Bell-Shaped Curves) Based on Expected %CV and Confidence Level: Concentrations, above that associated with the observed E_{\max} , that exhibit fold induction that is < 70% of the observed E_{\max} (i.e. > 30% decrease) can be excluded from curve fitting, assuming 30% CV and a 95% 2-sided confidence interval. Excluding these data points converts a “bell-shaped” curve to a curve where E_{\max} is not achieved (See footnote 5, below). Note: in general, excluding “outliers” using traditional tests (e.g. Grubb’s) is not recommended for triplicate data due to the small sample size (Laio, 2010).

³Fit fold Induction Data with Model of Choice: 3 or 4-parameter logistic, E_{\max} , hyperbolic, and sigmoidal 3-parameter models all provide similar estimates of E_{\max} and EC_{50} when the concentration range tested adequately characterizes the minimum and maximum fold induction.

⁴Reject Estimated E_{\max} values > 130% of the Maximum Observed E_{\max} : Assuming 30% CV and a one-sided 95% confidence interval, E_{\max} estimates > 130% of the maximum observed fold induction are rejected.

⁵Recommended Approaches for Addressing Curves where Maximum Fold induction is Not Achieved: Four methods are proposed for estimating induction parameters where the maximum fold induction is not achieved (defined as the fitted E_{\max} > 130% of observed maximum fold induction: 1) Constrain fit to observed E_{\max} and report E_{\max} and EC_{50} as > fitted values; 2) Fit data using Sigmoidal 3P fit, which approximates E_{\max} to observed E_{\max} and over-estimates potency, and report E_{\max} and EC_{50} as > fitted values; 3) Use the initial slope to estimate E_{\max}/EC_{50} and DDI risk using R3 equation; 4) Utilize shorter incubation duration (24 h). A shorter incubation may alleviate tolerability issues following prolonged exposure to test article at high concentrations and enable better characterization of the concentration-response curve.

Tables

Table 1: Summary of EC₅₀ and E_{max} estimates determined by 7 IWG member laboratories following treatment of human hepatocytes with prototypical CYP inducers for 6, 12, 24, 48 or 72 hours. ND = not determined.

Isoform	INDUCER	Parameter	Median and Range (Max to Min) EC ₅₀ and E _{max} Estimates at Each Time Point									
			6		12		24		48		72	
			mRNA	Activity	mRNA	Activity	mRNA	Activity	mRNA	Activity	mRNA	Activity
CYP1A2	Omeprazole	Median EC ₅₀ (μM) (n)	6.2 (3)	6.0 (4)	10.2 (4)	5.9 (3)	15 (6)	6.6 (5)	13 (6)	13 (6)	14 (7)	40 (7)
		Max – Min	3.9 - 9.1	2.1 - 12	4.9 - 20	4.6 - 7.8	7.0 - 62	5.8 - 13	9.1 - 36	5.7 - 200	7.1 - 35	3.8 - 100
	Phenobarbital	Median E _{max} (fold)	8.2	1.6	8.5	4.0	35	6.8	57	13	45	18
		Max - Min	1.9 - 20	1.4 - 2.7	3.9 - 47	1.9 - 5.5	12 - 133	6.6 - 23	17 - 170	9.4 - 59	28 - 76	9.5 - 59
CYP2B6	Efavirenz	Median EC ₅₀ (μM) (n)	3.6 (7)	1.6 (1)	2.9 (5)	ND (0)	1.9 (5)	ND (0)	1.4 (6)	0.76 (2)	1.1 (6)	4.0 (2)
		Max – Min	1.3 – 5.8	ND	0.40 - 23	ND	0.6 - 7.5	ND	0.4 – 3.1	0.5 - 1	0.5 - 8.4	3.9 - 4.0
	Phenobarbital	Median E _{max} (fold)	6.4	0.63	9.3	ND	7.6	ND	9.5	3.7	9.4	5.3
		Max - Min	1.3 - 18	ND	3.1 - 21	ND	2.8 - 32	ND	4.2 - 21	2.4 - 5	1.6 - 21	3.8 - 6.8
	Rifampicin	Median EC ₅₀ (μM) (n)	450 (7)	380 (4)	340 (6)	560 (5)	260 (7)	630 (5)	230 (6)	510 (6)	305 (7)	500 (5)
		Max – Min	120 - 1600	160 - 25000	127 - 1460	310 - 800	120 - 1900	410 - 1400	150 - 560	140 - 4700	28 - 1100	62 - 3500
CYP2C9	Rifampicin	Median E _{max} (fold)	12	2.0	14	2.6	18	8.1	25	27	19	40
		Max - Min	1.3 - 22	1.5 - 2.8	5.1 - 33	1.3 - 10	2.6 - 58	2.2 - 29	6.4 - 49	10 - 40	8.4 - 61	7.7 - 41
CYP3A4	Efavirenz	Median EC ₅₀ (μM) (n)	1.5 (6)	2.0 (4)	1.1 (1)	2.9 (4)	0.80 (6)	1.2 (6)	0.65 (6)	1.8 (6)	0.62 (6)	1.1 (6)
		Max – Min	0.2 - 2.3	0.2 - 3.9	NA	0.2 - 4.3	0.1 - 1.3	0.18 - 3.5	0.3 - 1.8	0.73 - 3.7	0.5 - 1.4	0.5 - 7.8
	Rifampicin	Median E _{max} (fold)	4.8	1.2 - 2.3	8.75	4.9	6.9	3.7	9.3	11	11	11
		Max - Min	1.3 - 15	1.2 - 2.3	5.3 - 17	1.4 - 8.9	1.9 - 17	1.6 - 14	5.9 - 13	5.6 - 16	5.1 - 15	8.1 - 13
CYP2C9	Rifampicin	Median EC ₅₀ (μM) (n)	0.2 (1)	-	0.29 (3)	-	1.2 (3)	-	0.20 (4)	-	0.10 (6)	-
		Max – Min	NA	-	0.1 - 0.4	-	0.11 - 8.7	-	0.07 - 0.9	-	0.08 - 1.1	-
CYP3A4	Efavirenz	Median E _{max} (fold)	1.3	-	1.9	-	2.7	-	3.0	-	3.3	-
		Max - Min	1.3 - 1.4	-	1.8 - 5.5	-	1.8 - 7.8	-	2.2 - 6.6	-	2.2 - 4.2	-
	Rifampicin	Median EC ₅₀ (μM) (n)	4.6 (4)	2.3 (3)	8.4 (4)	11 (4)	7.2 (6)	13 (4)	8.2 (4)	4.77 (4)	3.9 (5)	7.90 (4)
		Max – Min	3.5 - 6.5	2.0 - 6.5	5.1 - 18	3.5 - 16	3.1 - 62	4.6 - 42	1.0 - 18	0.78 - 13.5	2.0 - 19	0.34 - 11
CYP3A4	Rifampicin	Median E _{max} (fold)	2.2	1.8	8.8	5.9	11	13	14	11.6	15	13.1
		Max - Min	1.2 - 25	1.7 - 2.9	3.5 - 39	2.7 - 16	4.8 - 30	4.7 - 42	3.7 - 31	10 - 120	9.7 - 38	6.1 - 140
CYP3A4	Rifampicin	Median EC ₅₀ (μM) (n)	0.49 (5)	ND (0)	0.50 (6)	0.7 (5)	0.65 (7)	0.37 (6)	0.43 (6)	0.28 (6)	0.38 (7)	0.23 (6)
		Max – Min	0.06 - 0.76	ND	0.38 - 3.8	0.12 - 10	0.14 - 1.6	0.10 - 40	0.08 - 1.1	0.06 - 2	0.04 - 9.1	0.02 - 0.77
CYP3A4	Rifampicin	Median E _{max} (fold)	5.7	1.5	15	3.5	21	5.0	21	8.2	20	10.2
		Max - Min	2.3 - 31	ND	3.5 - 44	1.1 - 6.6	4.8 - 50	2.2 - 15	10 - 50	5.4 - 29	5.8 - 67	5.3 - 31

Table 2: Summary of % Positive Induction Response (> 2 -fold E_{\max}) at 6, 12, 24, 48, or 72 hours following treatment with prototypical inducers. Each value represents the % of donors yielding an $E_{\max} > 2$ -fold at each time point.

ISOFORM	INDUCER	% of Donors with > 2 –Fold Induction At Each Time Point									
		6		12		24		48		72	
		mRNA	Activity	mRNA	Activity	mRNA	Activity	mRNA	Activity	mRNA	Activity
CYP1A2	Omeprazole	67	25	75	67	100	100	100	100	100	100
	Phenobarbital	40	50	80	75	60	75	67	100	57	86
CYP2B6	Efavirenz	86	0	100	0	100	0	100	100	83	100
	Phenobarbital	86	50	100	60	100	100	100	100	100	100
	Rifampicin	67	50	100	75	83	83	100	100	100	100
CYP2C9	Rifampicin	0	ND	33	ND	75	ND	100	ND	100	ND
CYP3A4	Efavirenz	60	33	100	100	100	100	100	100	100	100
	Rifampicin	100	0	100	80	100	100	100	100	100	100
		% Donors with > 10 –Fold Induction At Each Time Point									
	Rifampicin	20	0	83	0	100	33	86	17	86	50

Table 3: Summary of Average Fold Error (AFE) Comparing E_{\max} , EC_{50} , or E_{\max}/EC_{50} at Earlier Timepoints (6, 12, 24, or 48) to 72 hr. AFE's were summarized for each CYP isoform and respective inducers: CYP1A1 (omeprazole, phenobarbital), CYP2B6 (efavirenz, phenobarbital, rifampicin), CYP2C9 (rifampicin), CYP3A4 (efavirenz, rifampicin).

Average Fold Error (AFE) of Parameter Estimate (E_{\max} , EC_{50} , or E_{\max}/EC_{50}) determined at 6, 12, 24, or 48hr Compared to Estimate at 72hr									
Parameter Estimate	CYP Isoform	6hr		12hr		24hr		48hr	
		mRNA	Activity	mRNA	Activity	mRNA	Activity	mRNA	Activity
E_{\max} AFE (n)	CYP1A2	0.33 (7)	0.10 (6)	0.42 (8)	0.35 (7)	0.77 (10)	0.48 (8)	0.89 (10)	0.81 (13)
	CYP2B6	0.42 (20)	0.10 (7)	0.59 (15)	0.21 (9)	0.64 (18)	0.45 (10)	0.96 (18)	0.90 (13)
	CYP2C9	0.49 (2)	-	0.84 (3)	-	0.94 (4)	-	1.0 (4)	-
	CYP3A4	0.29 (9)	0.22 (4)	0.76 (9)	0.30 (9)	0.90 (12)	0.55 (10)	0.97 (12)	0.90 (10)
	Overall AFE (n)	0.36 (38)	0.13 (17)	0.60 (35)	0.27 (25)	0.76 (44)	0.50 (28)	0.95 (44)	0.87 (36)
	% Within 2-fold (n)	39 (15)	0 (0)	51 (18)	28 (7)	68 (30)	36 (10)	86 (38)	89 (32)
EC_{50} AFE (n)	CYP1A2	0.93 (5)	0.32 (6)	0.64 (8)	1.1 (7)	1.24 (10)	0.56 (7)	0.75 (10)	0.94 (12)
	CYP2B6	1.82 (19)	1.2 (8)	1.99 (12)	1.3 (9)	1.30 (18)	1.0 (11)	1.07 (18)	1.0 (12)
	CYP2C9	2.0 (1)	-	1.1 (3)	ND	2.4 (3)	-	0.70 (4)	ND
	CYP3A4	1.8 (8)	1.1 (3)	2.0 (9)	4.1 (9)	1.6 (12)	2.7 (10)	1.1 (10)	1.5 (10)
	Overall AFE (n)	0.36 (38)	0.13 (17)	0.60 (35)	0.27 (25)	0.76 (44)	0.50 (28)	0.95 (44)	0.87 (36)
	% Within 2-fold (n)	42 (14)	35 (6)	44 (14)	32 (8)	49 (21)	21 (6)	70 (30)	44 (15)
E_{\max}/EC_{50} AFE (n)	CYP1A2	0.32 (5)	0.34 (4)	0.32 (8)	0.54 (5)	0.35 (10)	0.68 (7)	0.45 (8)	0.84 (11)
	CYP2B6	0.21 (18)	0.083 (8)	0.20 (11)	0.16 (9)	0.52 (17)	0.42 (10)	0.95 (16)	0.94 (13)
	CYP2C9	0.19 (1)	-	0.77 (3)	-	0.43 (3)	-	1.4 (4)	-
	CYP3A4	0.22 (7)	0.071 (2)	0.37 (9)	0.076 (8)	0.55 (12)	0.20 (10)	0.94 (10)	0.60 (10)
	Overall AFE (n)	0.36 (38)	0.13 (17)	0.60 (35)	0.27 (25)	0.76 (44)	0.50 (28)	0.95 (44)	0.87 (36)
	% Within 2-fold (n)	19 (6)	14 (2)	48 (15)	18 (4)	55 (23)	41 (11)	87 (33)	59 (20)

Table 4: Two-sided large confidence intervals, based on a known %CV, for an observed E_{\max} of 100 (n=3).

2-Sided Confidence Interval Level	% CV	Observed E_{\max} Fold induction	Lower Limit (Observed Fold Induction)	Higher Limit (Fitted E_{\max})
0.95	0.1	100	88	112
	0.2	100	76	124
	0.3	100	67	133
0.900	0.1	100	90	110
	0.2	100	80	120
	0.3	100	72	128
0.800	0.1	100	92	108
	0.2	100	85	115
	0.3	100	78	122

Table 5: Comparison of AICc, E_{\max} , and EC_{50} estimates determined for CYP3A4 induction mediated by rifampicin or efavirenz. Fold induction data was fitted from representative mean data generated from a single laboratory. The corresponding plots for these fits are shown in Figure 9A (rifampicin) and 9B (efavirenz). 3P = Logistic 3-Parameter; 4P = Logistic 4-Parameter; SIG = Sigmoidal 3-Parameter; E_{\max} = E_{\max} (Hill); HYP = Hyperbolic (One-Site)

Rifampicin					
	3P	4P	SIG 3P	E_{\max}	HYP
E_{\max}	19.5	18.5	17.7	18.8	19.5
EC_{50} (μM)	0.340	0.328	0.287	0.303	0.328
AICc	20.99	10.51	19.52	17.49	18.26
AICc Delta From Lowest	10.5	0.0	9.0	7.0	7.8
AICc Weight	0.00497	0.937	0.0104	0.0286	0.0194

Efavirenz					
	3P	4P	SIG	E_{\max}	HYP
E_{\max}	35.9	19.2	15.1	49.1	30.4
EC_{50} (μM)	14.5	4.94	3.60	26.5	10.2
AICc	-4.18	-13.2	-14.9	1.28	-1.36
AICc Delta From Lowest	10.7	1.7	0.0	16.2	13.6
AICc Weight	0.00327	0.296	0.700	0.000213	0.000799

Table 6: Comparison of DDI risk assessment for efavirenz using various approaches to estimate E_{\max} and EC_{50} . F2 = concentration that elicits 2-fold induction. R3 was calculated using equation 10 (for logistic and sigmoidal 3P fits) or equation 11 (initial slope method).

Modeling Approach	E_{\max}	EC_{50}	E_{\max}/EC_{50}	F2	R3
Logistic 3P	38.5	16.5	2.327	0.45	0.27
Sigmoidal 3P	15.1	3.60	4.197	0.62	0.20
Logistic 3P with E_{\max} Constrained to Observed E_{\max}	15.1	3.1	> 4.87	> 0.24	0.19
Initial Slope	NA	NA	1.5	ND	0.35

Table 7: Summary of average fold error of R3 determined using E_{\max} and EC_{50} (Equation 10) estimated using Sigmoidal-3-Parameter fit compared to initial slope estimation of E_{\max}/EC_{50} (Equation 11)

Inducer	CYP	R3 (E_{\max} and EC_{50})	R3 (Initial Slope)	Average Fold Error
Omeprazole	1A2	0.226 ± 0.104	0.333 ± 0.145	0.685
Efavirenz	3A4	0.202 ± 0.030	0.298 ± 0.0657	0.685
Efavirenz	2B6	0.243 ± 0.161	0.249 ± 0.168	0.955
Rifampicin	3A4	0.249 ± 0.223	0.201 ± 0.0733	0.823
Overall				0.830

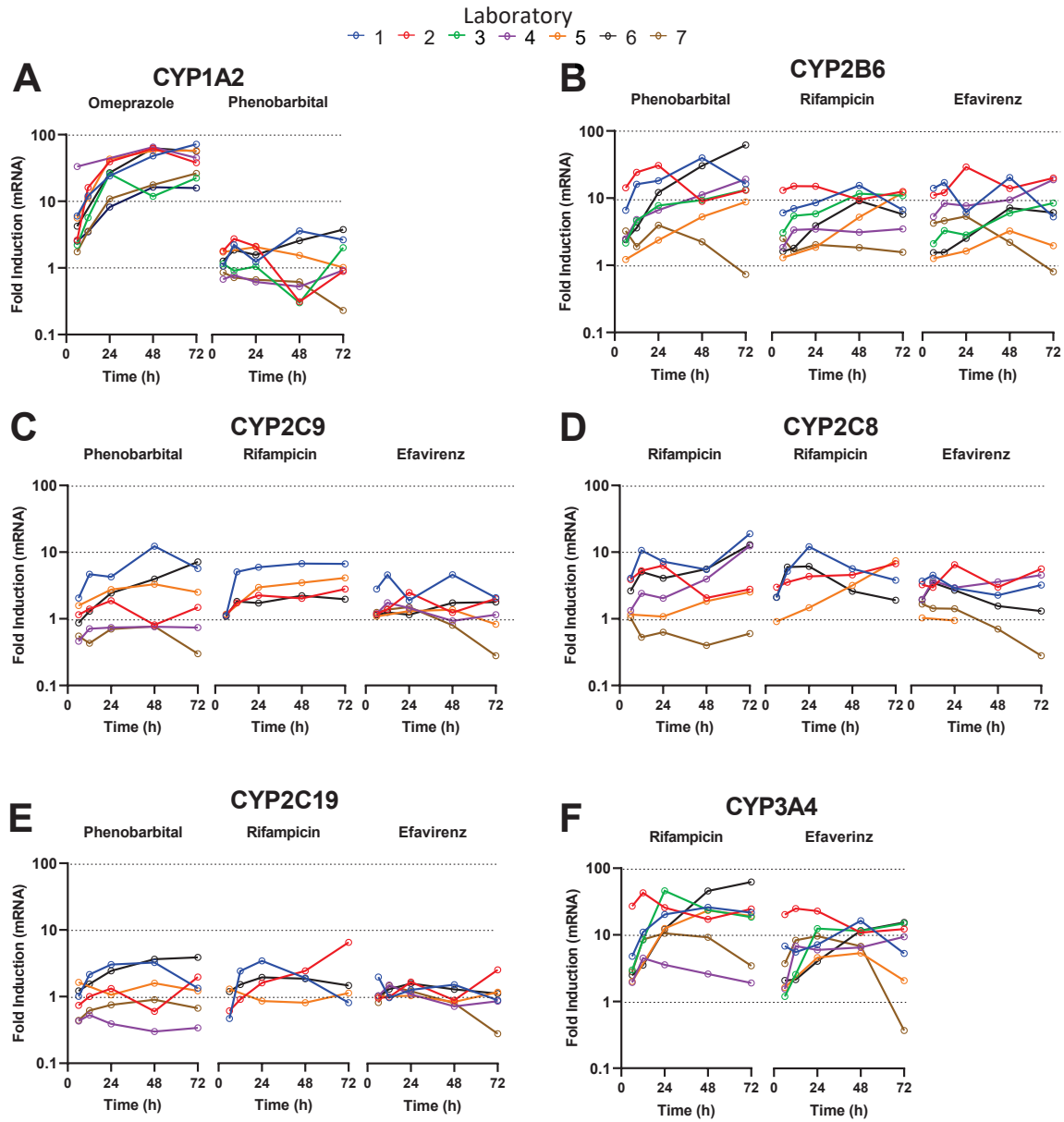


Figure 1

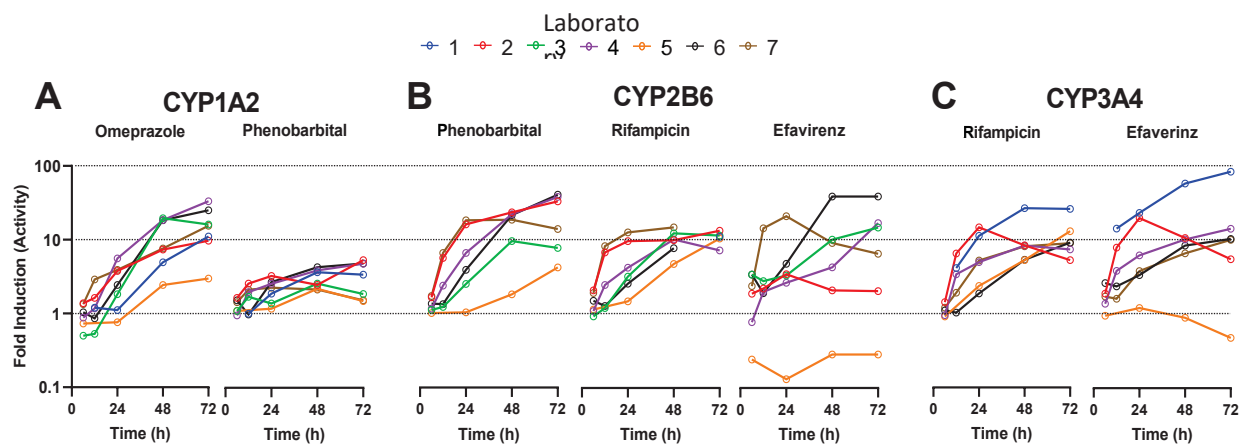


Figure 2

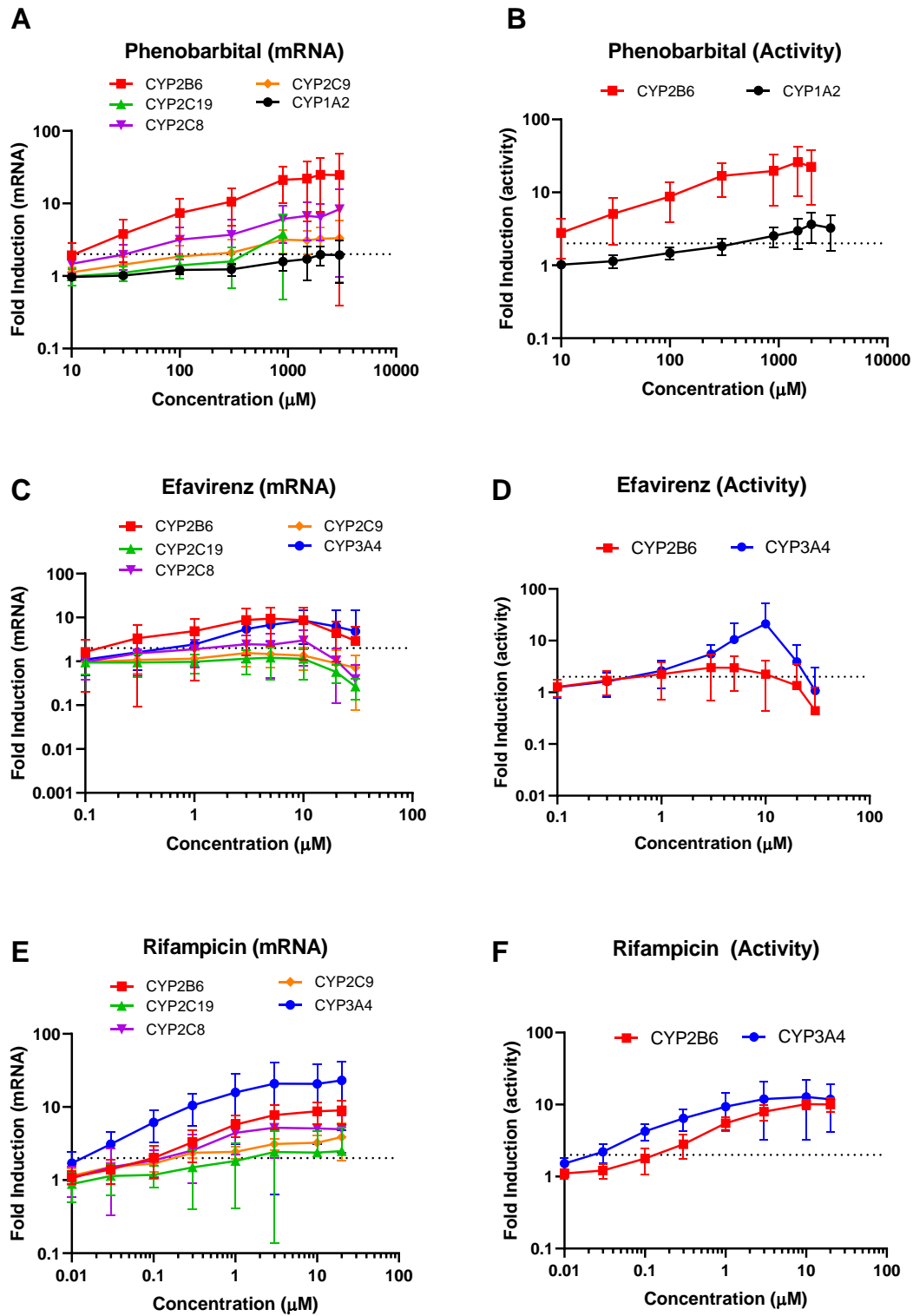


Figure 3

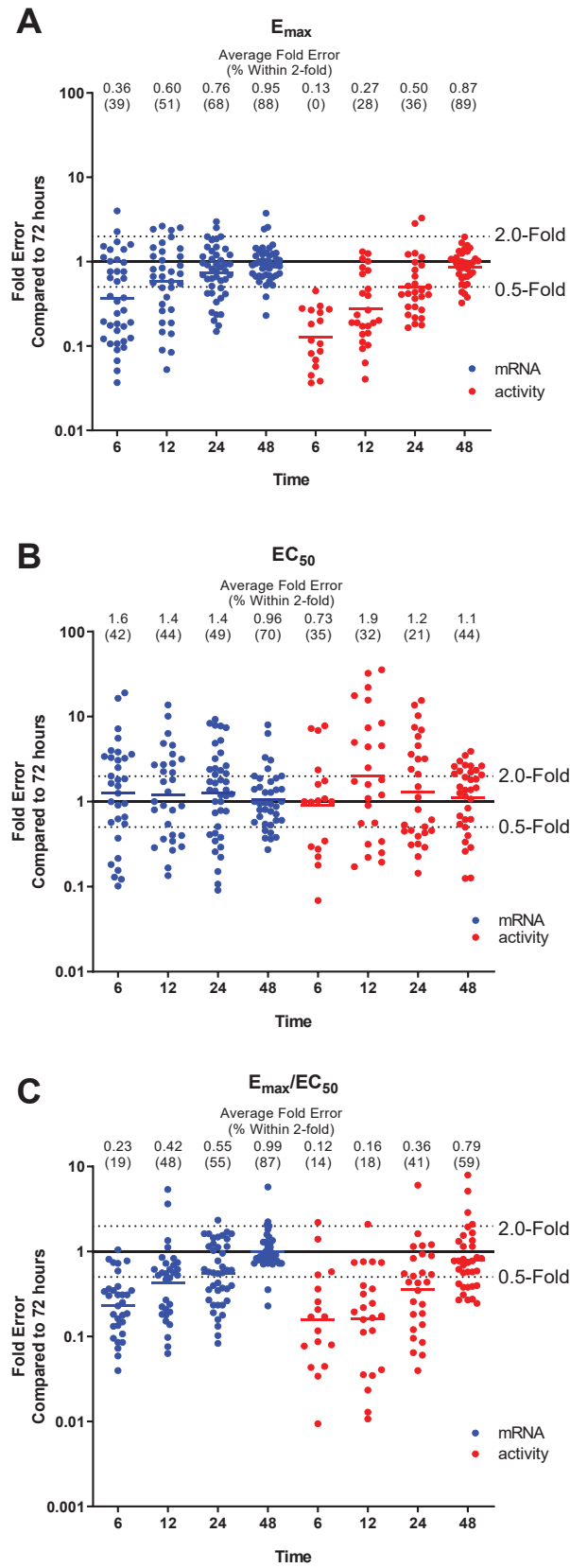


Figure 4

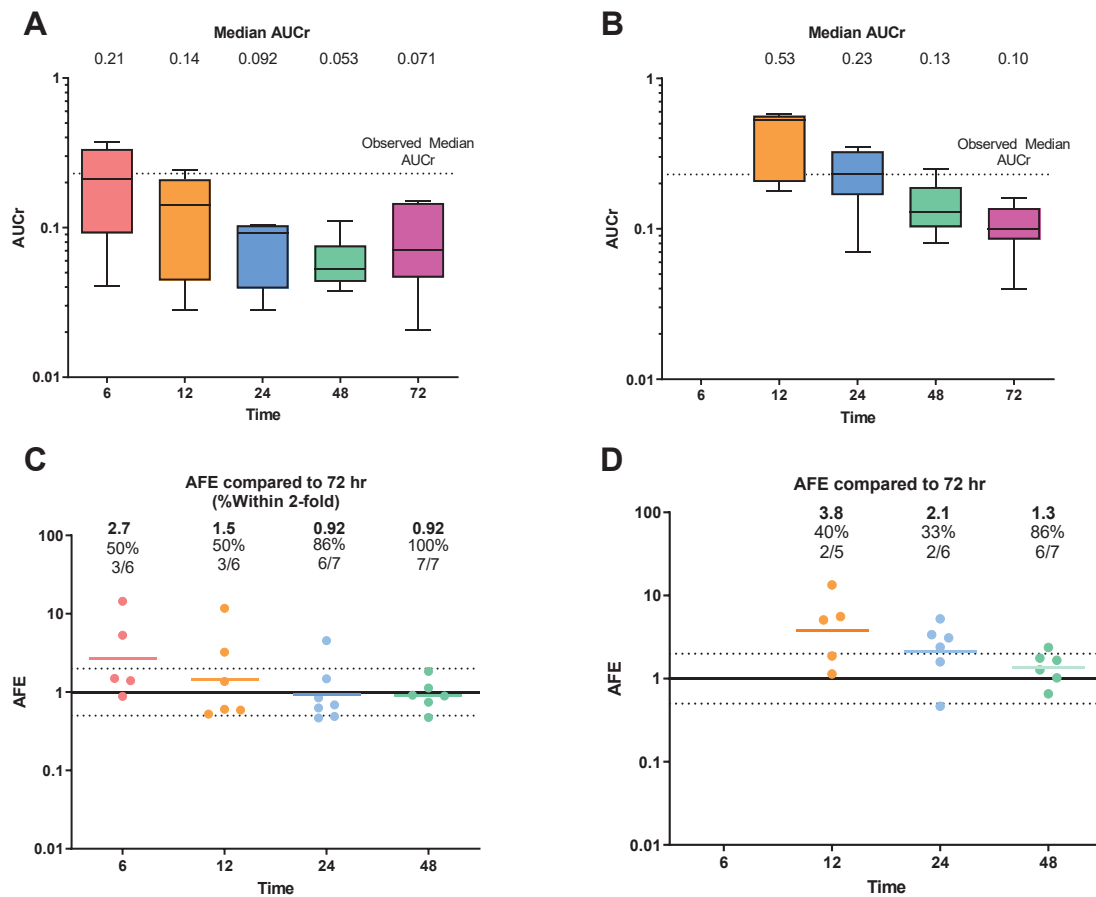


Figure 5

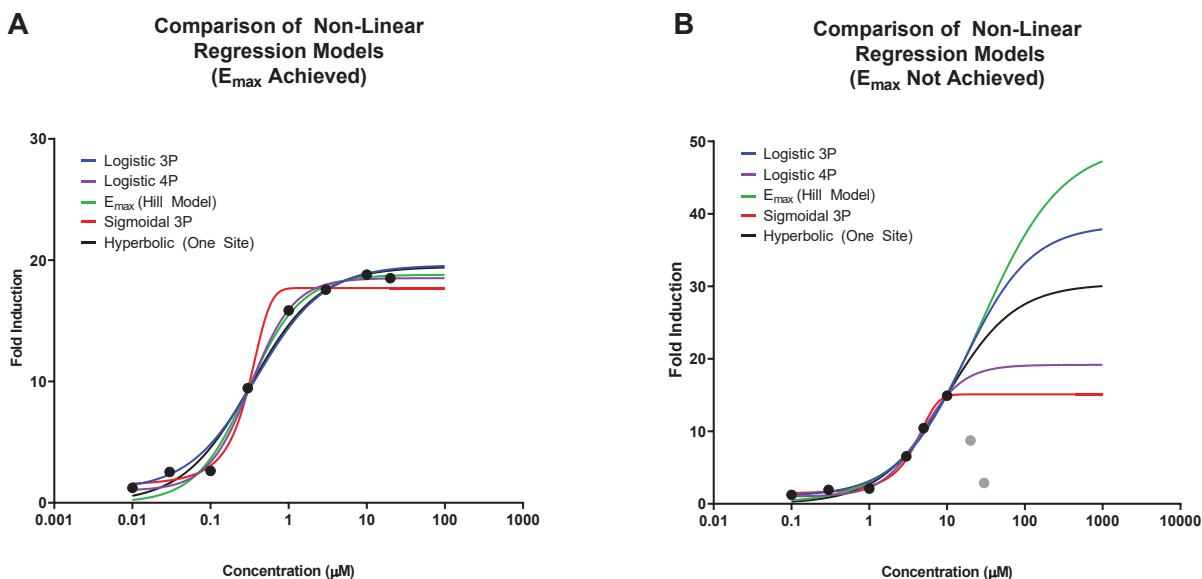


Figure 6

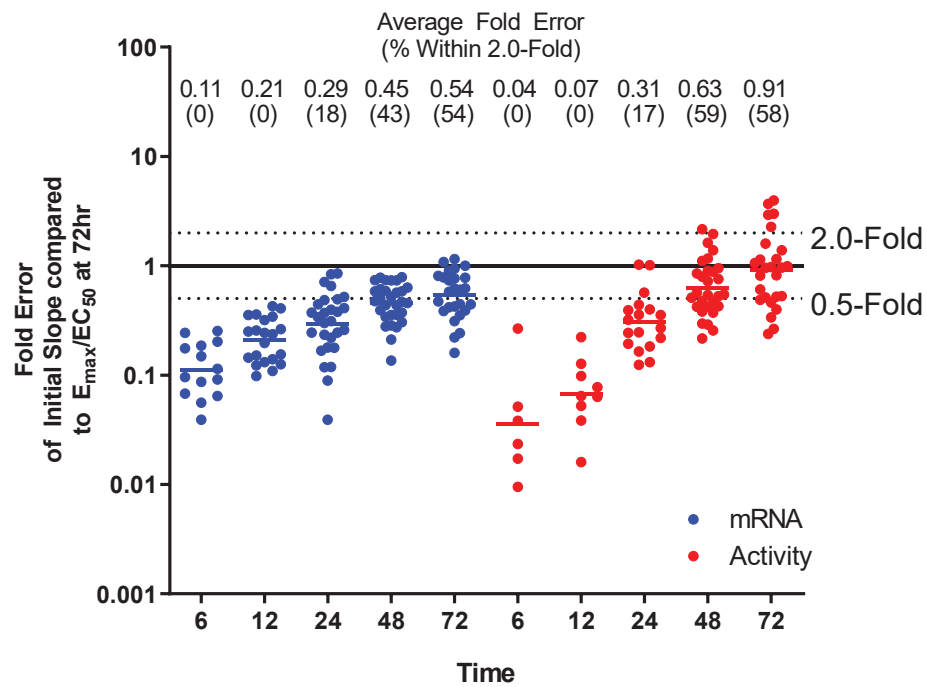


Figure 7

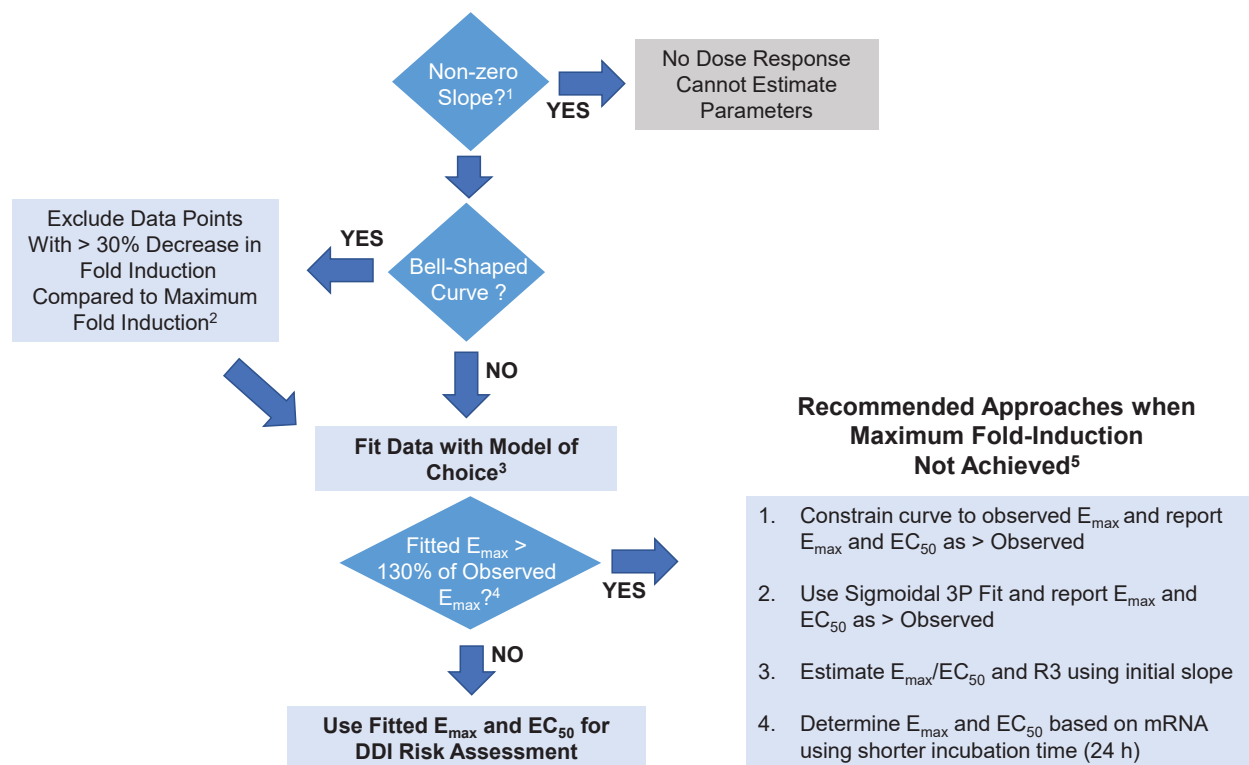
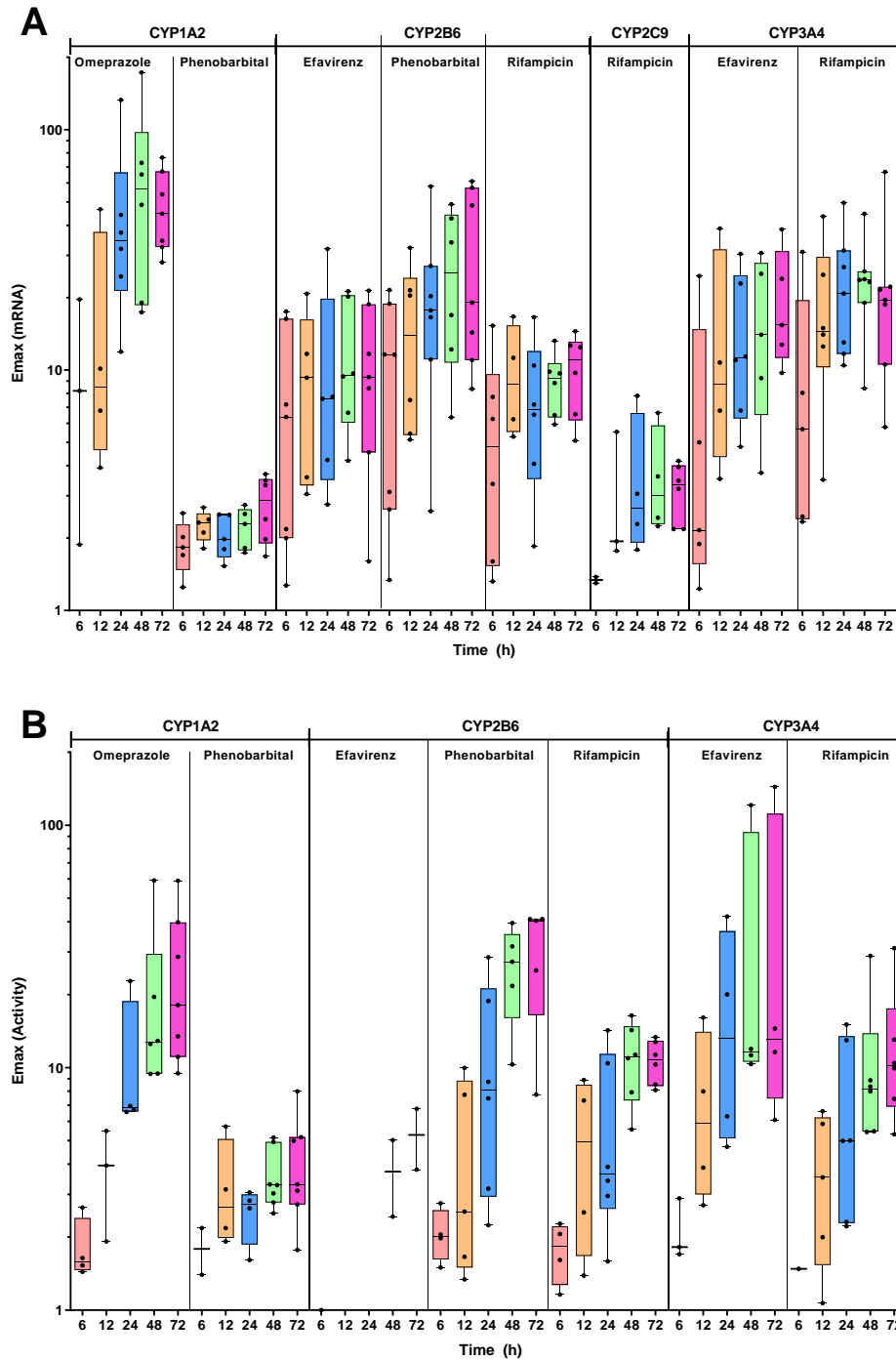


Figure 8

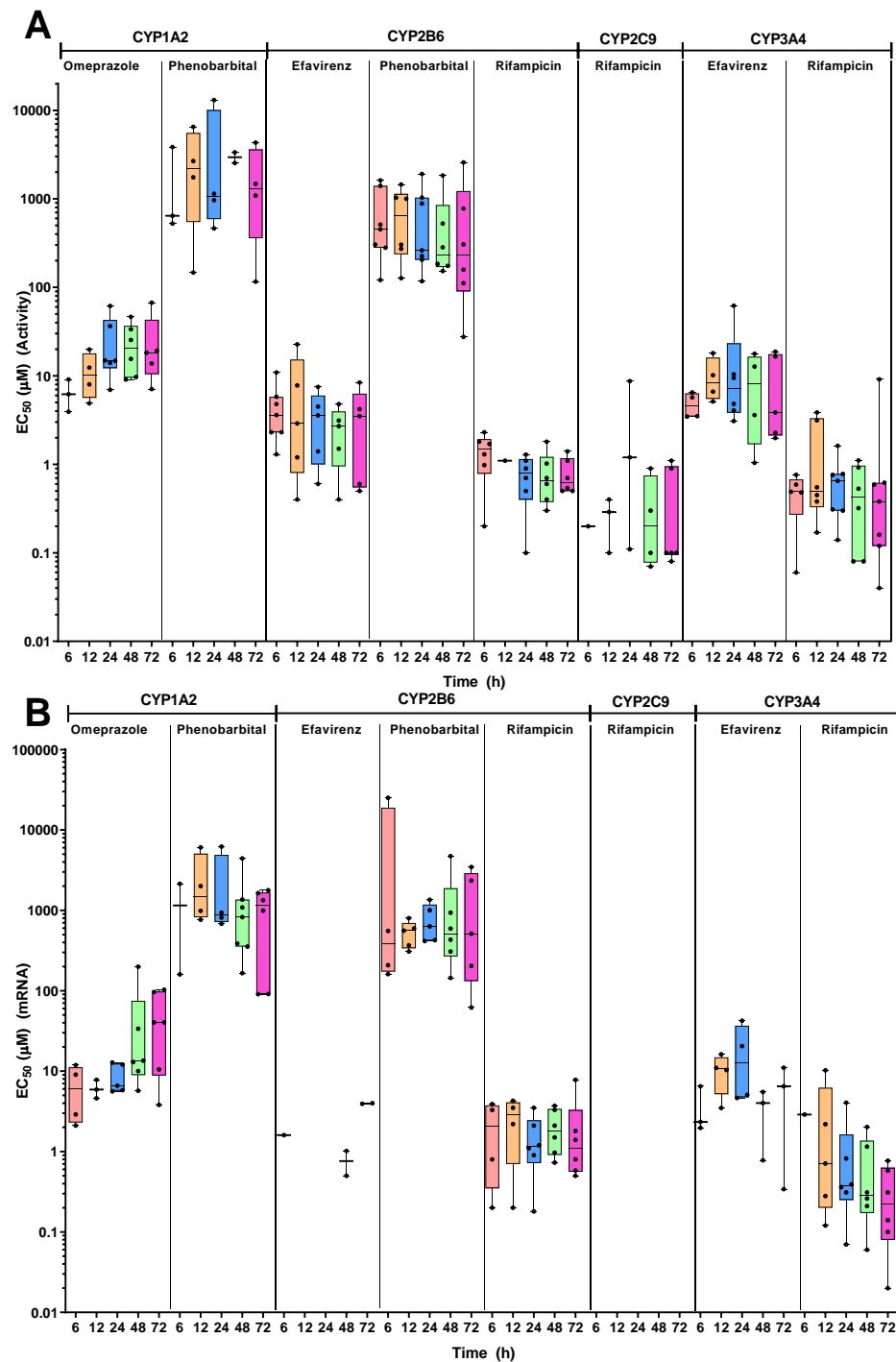
Considerations from the Innovation and Quality Induction Working Group in Response to Drug-Drug Interaction Guidance from Regulatory Agencies: Guidelines on Model Fitting and Recommendations on Time Course for In Vitro CYP Induction Studies Including Impact on Drug Interaction Risk Assessment

Simon G. Wong, Diane Ramsden, Shannon Dallas, Conrad Fung, Heidi J. Einolf, Jairam Palamanda, Liangfu Chen, Theunis C. Goosen, Y. Amy Siu, George Zhang, Donald Tweedie, Niresh Hariparsad, Barry Jones, and Phillip D. Yates.

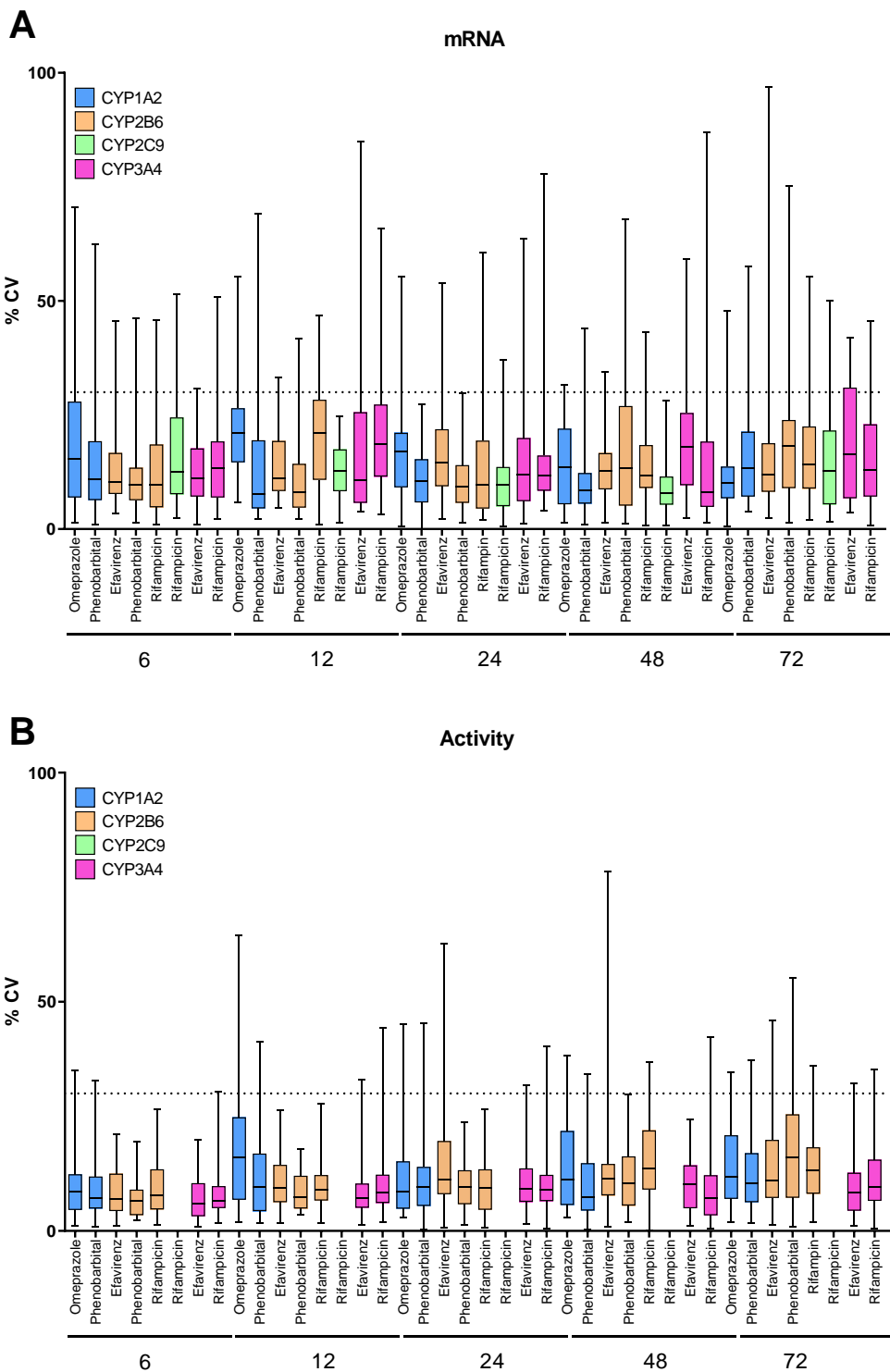
SUPPLEMENTAL INFORMATION



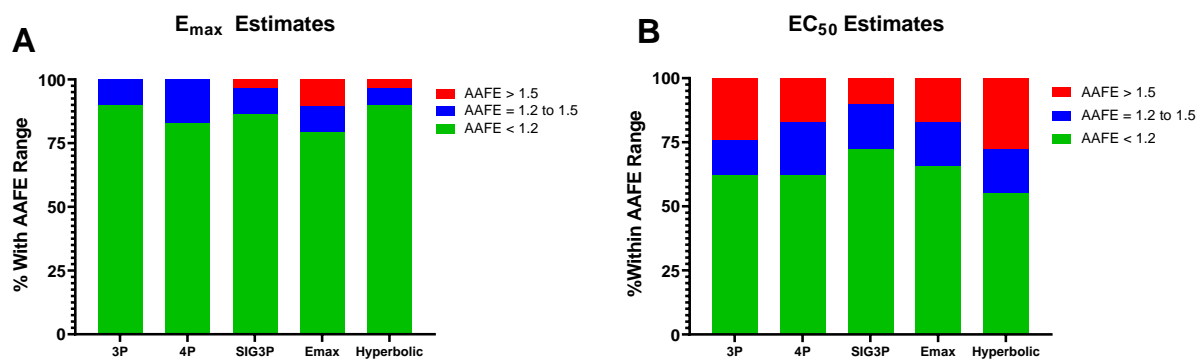
Supplemental Figure 1: Box and Whisker plots of model estimates of E_{max} for mRNA(A) or activity (B) following treatment of human hepatocytes with omeprazole, phenobarbital, efavirenz, or rifampicin for 6, 12, 24, 48, or 72 hr. Each solid circle represents the mean of triplicate determinations from a single experiment conducted at each laboratory.



Supplemental Figure 2: : Box and Whisker plots of model estimates of EC_{50} for mRNA(A) or activity (B) following treatment of human hepatocytes with omeprazole, phenobarbital, efavirenz, or rifampicin for 6, 12, 24, 48, or 72 hr. Each solid circle represents the mean of triplicate determinations from a single experiment conducted at each laboratory.



Supplemental Figure 3: Overall average %CV (for triplicate fold induction, across all donors) for each prototypical inducer at each time point, for mRNA and activity. Dotted line illustrates 30% CV.



Supplemental Figure 4: Comparison of the absolute average fold error (AAFE) between the best model estimates (determined using the model with the lowest AICc) for E_{max} (A) or EC₅₀ (B) and each respective model fit, for all CYP inducers and isoforms.

Supplementary Tables

Supplemental Table 1. Donor demographics for human hepatocyte donors

Hepatocyte donor #	Vendor	Gender/Age (yrs)	Matrigel overlay (Y/N)
385	Corning	Male/39	Y
Hu8123	Cellz Direct/In vitro life technologies	Male/48	N
HUM4080	Lonza	Female/47	Y
FOS	BioIVT	Male/34	Y
YEM	BioIVT	Female/46	N
BHL	BioIVT	Male/28	N
NHI	BioIVT	Male/48	N
Hu1624	Thermo Fisher	Female/72	N
BPB	BioIVT	Female/42	N

Supplemental Table 2. Inducer Test Concentrations

Inducer	Test Concentrations (μ M)
efavirenz	0.1 0.3, 1, 3, 5, 10, 20, 30
omeprazole	1, 3, 10, 20, 30, 50, 100
phenobarbital	10, 30, 100, 300, 900, 1500, 3000
rifampicin	0.01, 0.03, 0.1, 0.3, 1, 3, 10, 20